약학박사학위논문

지질대사 이상 질환에서 핵 수용체 **LXR**의 역할 및 기전에 대한 연구

Role of liver X receptors in the pathogenesis of lipid metabolism disorders

2013년 2월

서울대학교 대학원

약학과 병태생리학전공

나 태 영

ABSTRACT

Role of liver X receptors in the pathogenesis of lipid metabolism disorders

Tae Young Na

Majoring in Pathophysiology

Department of Pharmacy Graduate School

Advisor: Prof. Mi-Ock Lee

The liver X receptors (LXRs) are nuclear receptors that are activated by endogenous oxysterols, oxidized derivatives of cholesterol. The LXRs are involved in the process of reverse cholesterol transport which is the process by which the lipoprotein particle, HDL, carries cholesterol from the peripheral tissues to the liver and play a critical role in metabolic abnormalities, including insulin resistance, obesity, dyslipidemia and hypertention.

The first part of this study describes the role of LXRs in hepatitis B virus X

protein-induced lipogenesis in hepatitis B virus-associated hepatocellular carcinoma. Several studies have suggested that infection by HBV genotypes B is associated with an increased risk of HCC; however, the molecular mechanism by which HBV induces events leading to HCC has not been clearly elucidated. In this study, HBx induced expression of LXRs and its lipogenic target genes, which was accompanied by the accumulation of lipid droplets. RNA interference of LXRα or β expression effectively blocked the amount of lipid droplets as well as the expression of the lipogenic genes, indicating that the HBx-induced lipogenesis was LXR-dependent. HBx and LXRα are physically associates in the nucleus. HBx enhanced transactivation function of LXRα by recruiting CBP to the SREBP-1c promoter. Furthermore, the expression of LXRs was significantly increased in the liver of HBx-transgenic mice. Finally, there was a significant increase in the expression of LXRα and its lipogenic target genes in human HBV-associated HCC specimens. These results suggest a novel association between HBx and LXR-induced hepatic lipogenesis, which may constitute a pivotal molecular mechanism underlying the development of HBV-associated HCC.

The second part of this study describes the role of cross-talk between LXRα and HIF-1α for the formation of triglyceride-rich foam cells during the development of atherosclerosis. Atherosclerosis is characterized by subendothelial accumulation of lipid-rich macrophages, called foam cells. Hypoxic conditions in the atherosclerotic lesions contribute to the formation of these lipid-loaded macrophages. The liver X receptor is a regulator of lipid metabolism in many tissues, however, role of LXRα in the foam cell formation is not known. In this study, the expression of LXRα was time-dependently induced under hypoxia in human primary macrophages and RAW 264.7 cells. Knockdown of HIF-1α using si-RNA completely abolished the induction of LXRα and its target genes indicating that the induction of LXRα was HIF-1α dependent. TO901317, an activator of LXRα, enhanced the expression level and the transcriptional activity of HIF-1α, which was also decreased by knockdown of LXRα. Second, LXRα increased HIF-1α protein stability through a physical interaction between the ligand binding domain of LXRα and the oxygen-dependent degradation domain of HIF-1α. Third, the activation of HIF-1α or LXRα synergistically induced

triglyceride accumulation in the macrophages. Finally, LXRα and HIF-1α were codistributed in the macrophages of atherosclerotic arteries obtained from patients. These results suggest that the positive feedback regulation of transcriptional induction and protein stability of LXRα and HIF-1α may have an important impact for foam-cell formation and the development of atherosclerotic lesions.

Taken together, it is suggested that that the molecular mechanism of LXR activation may turn on a vicious cycle of lipid production and inflammation in the lipid metabolism disorder.

Keywords : Hepatitis B Virus, HBx, Liver X Receptor, Hepatocellular carcinogenesis, Hepatosteatosis, Hypoxia, HIF-1α, Foam cell, Atherosclerosis

Student ID : 2006-21966

CONTENTS

LIST OF FIGURES

ABBREVIATIONS

HBV, Hepatitis B virus

HBx, HBV- X protein

LXR, Liver X Receptor

HIF-1, Hypoxia inducible factor-1

VEGF, Vascular endothelial growth factor

DFO, Desferrioxamine

$CoCl_2$, Cobalt chloride

LXRE, Liver X Receptor response element

SREBP-1c, Sterol regulatory element binding protein-1c

PPAR, Peroxisome proliferators-activated receptor

FAS, Fatty acid synthase;

PHD, Prolyl hydroxylases

β-gal, β-galactosidase

PBS, Phosphate-buffered saline

AS, Antisense

CBP, CREB binding protein

CHIP, Chromatin immunoprecipitation

ChREBP, Carbohydrate-responsive element-binding protein

CMV, Cytomegalovirus

DAPI, 4,6-diaminidino-2-phenylindole

Doxy, Doxycycline

FAS, Fatty acidsynthase

Gal, Galactosidase

HA, Hemagglutinin

HCV, Hepatitis C virus

IP, Immunoprecipitation

SCD-1, Stearoyl– coenyzme A desaturase-1

Ub, Ubiquitination

I. INTRODUCTION

1. Biological role of Liver X Receptors

1.1. The nuclear receptors LXRα and LXRβ as the NR family of transcription factors

The 48 members of the NR family in humans are master regulators of transcriptional programs that integrate the homeostatic control of almost all biological processes including development, reproduction, cell growth, metabolism, immunity and inflammation.

LXRs, Liver X receptors, are ligand-activated transcription factors that belong to the nuclear receptor superfamily. They were first identified in 1994 by screening a rat liver cDNA library (1). LXRs were initially classified as orphan nuclear receptors because their natural ligands were unknown. In the following years identification of several physiological ligands has "adopted" these receptors. Two different genes have been described, LXRα (NR1H3) and LXRβ (NR1H2) that are highly related and share

~78% identity of their amino acid sequences in both DNA and ligand-binding domains (2). High expression of LXRa is restricted to spleen, liver, adipose tissue, intestine, kidney and lung whereas LXRb is expressed in all tissues examined (1, 3). Two LXR subtypes, LXRα (NR1H3) and LXRβ (NR1H2), have been identified, that form heterodimers with the 9-*cis* retinoid X receptor and bind to a specific DNA motif termed the LXR response element (LXRE) (1) (Fig. 1). LXRE consists of two idealized hexanucleotide sequences (AGGTCA) separated by four bases (DR-4 element). LXR/RXR is a so called "permissive heterodimer" that may be activated by ligands for either partner in an independent manner (1-3). In the absence of ligands LXR recruits complexes of corepressors that are exchanged with coactivators upon receptor activation (3).

1.2. Synthetic and natural exogenous LXR ligands

Two nonsteroid synthetic LXR agonists, T0901317 and GW3965, are commonly

used in experimental studies. T0901317 activates both LXRα and LXRβ with an EC_{50} of about 20 nM (3). GW3965 has a greater affinity toward LXRβ (EC_{50}=30 nM) than LXRα (EC_{50}=190 nM); however, the difference is too small to be useful in differentiating the two isoforms. Strictly speaking, T0901317 is not a completely selective LXR agonist because it also activates farnesoid X receptor (FXR) and pregnane X receptor (PXR) (4). However, the affinity of T0901317 for LXR is much higher than for PXR and FXR. Numerous oxysterols have been demonstrated to be potential endogenous ligands for LXR, such as 24-(*S*),25-epoxycholesterol, 24-(*S*)-hydroxycholesterol, 22-(*R*)-hydroxycholesterol, 25-hydroxycholesterol and 27-hydroxycholesterol. Although oxysterols are oxidized derivatives of cholesterols, cholesterol itself is not a ligand for LXR. These oxysterols are shown to be bind to LXR and stimulate transcriptional activity of LXR at physiological concentrations. (4,5).

1.3. Physiological functions of LXR

Physiological significance of individual LXR subtypes in the regulation of liver lipid metabolism was clearly shown in experiments where mice lacking either LXRα or LXRβ were challenged with high-cholesterol diet. Also, the importance of LXRs in physiological lipid and cholesterol metabolism also suggests that they may influence the development of metabolic disorders such as hyper-lipidemia and atherosclerosis. Evidence for these ideas has been observed by many studies that linked LXR activity to the pathogenesis of lipid disorder (6,7).

1.3.1. The role of LXR in lipid homeostasis

Liver X receptors (LXRs) is nuclear receptors that function as intracellular sensors for cholesterols. In response to ligands, this receptor induces transcriptional responses that maintain a balanced, finely tuned regulation of cholesterol and bile acid metabolism (6). LXRs also permit the efficient storage of carbohydrate- and fat-derived energy. The

systems suggest that they coevolved to constitute a highly sensitive and efficient system for the maintenance of total body fat and cholesterol homeostasis. Emerging evidence suggests that the tissue-specific action of this receptor is also crucial for the proper function of the cardiovascular, immune, reproductive, endocrine pancreas, renal, and central nervous systems (6-8). Together, LXRs represent potential therapeutic targets for the treatment and prevention of numerous metabolic and lipid-related diseases.

1.3.2. The role of LXR in inflammatory responses

Considerable evidence has identified both LXRα and LXRβ as anti-inflammatory transcription factors and physiological regulators of innate and adaptive immune responses, apoptosis and phagocytosis. Several studies linking LXRs to inflammatory responses revealed that LXRs antagonized cytokine-mediated expression of pro-inflammatory genes in macrophages; it was suggested that this is a consequence of transcriptional silencing of the proinflammatory transcription factor nuclear factor (NF)-*k*B (9). It was further demonstrated that LXRα regulates cell survival because

macrophages from LXRα -/- mice were more susceptible to bacterial infection and showed accelerated apoptosis. LXRs induced the expression of several anti-apoptotic factors while inhibiting that of pro-apoptotic factors, which explains this phenotype (10). Apoptotic cells generate cholesterol derivatives from breakdown of the cell membrane and then act as LXR agonists. It was shown that this stimulates apoptotic cell clearance by phagocytosis of cells engulfed by macrophages (10,11). These studies emphasize the pivotal regulatory function of LXRs in the control of anti-inflammatory response. However, administration of synthetic LXR ligands triggers the induction of the lipogenic pathway and elevates plasma triglyceride levels via SREBP-1. In Ldlr–/– mice, TO901317 increases mRNA for enzymes involved in fatty acid biosynthesis and produces massive hypertriglyceridemia (12-15). To complicate matters further, a proinflammatory role of LXRs was seen in primary human macrophages, which was in contrast to previous observations of LXRs as negative regulators of inflammatory gene expression (16,17). LXR activation augmented the production of inflammatory cytokines IL-12, TNF-α, IL-6, and IL-8 in human monocyte-derived immune cells (18).

1.3.3. The role of LXR in cancer

LXRs appear to have dual roles in cancer biology. First, LXRs suppress the proliferation of a variety of human cancer cells (19), and second, tumors produce LXR agonists (oxysterols) that inhibit a robust immune response as a mechanism of tumor escape from immune surveillance (20). At the molecular level, LXRs target the cell cycle at several points. LXRs reduce the expression of positive cell cycle regulators, whereas they increase the expression of cell-cycle inhibitors. Although LXRs control the expression and activity of regulators involved in all phases of the cell cycle, it seemed that the effect was particularly concentrated on G0/G1 cell cycle arrest (19). Studies in different mouse models confirmed the anti-proliferative effect by demonstrating that LXRs reduced the growth of xenografts from prostate cancer cells (21) and delayed the progression of androgen-dependent tumors towards androgen independence (22). It was reported that the ability of LXRs to control cholesterol metabolism affects the proliferation of lymphocytes. Lymphocytes depend on excess intracellular cholesterol for the synthesis of cellular membranes during the proliferative

events of clonal expansion, and activation of LXRs decreased intracellular levels of cholesterol via ABCA1/G1 cholesterol transporters, thereby decreasing proliferation (23). In line with this, the same study revealed that LXR knockout mice showed splenomegaly and an increase in the number of splenic lymphocytes compared to control mice. Liver regeneration after partial hepatectomy generates high levels of cholesterol for synthesis of new hepatocytes, thereby increasing intracellular oxysterol levels, which activate LXRs. Via induction of the ABC cholesterol transporters, activated LXRs deplete cellular cholesterol levels and thereby cell proliferation, and consequently inhibit liver regeneration (24). It was also shown that LXRs promote tumor cell death in glioblastomas, the most common malignancy of the brain (25). Activation of LXRs led to increased expression of ABCA1 and IDOL, triggering degradation of the LDL-R and thus decreasing cholesterol levels, thereby reducing tumor cell survival. DCs mediate antitumor activity after their CCR7-dependent migration to lymphoid organs, where they activate the adaptive T and B cell immune response. Tumors produce activators of LXRs that inhibit CCR7 expression in mature

DCs and therefore their migration to draining lymph nodes (20). Moreover, there was significantly less tumor growth in mice injected with immune cells from LXRa knockout mice.

1.3.4. The role of LXR in atherosclerosis

LXRs play a pivotal role in the pathogenesis of atherosclerosis by regulating important genes involved in lipid homeostasis and the inflammatory response (26-28). The expression of LXRs and their target genes has been found to be higher in the thoracic aorta (atheroprotective) than the aortic arch (atheroprone) (29). A similar gene expression profile is also seen in cultured endothelial cells subjected to laminar stress, which is commonly encountered in healthy arteries (29). SMCs regulate vascular contractive function and influence atherosclerotic development by modulating plaque stability (30). LXR agonists have been found to inhibit both vascular SMC proliferation and neointima formation in balloon-injured rat carotid arteries (31). LXRs also stimulate cholesterol efflux and inhibit the expression of pro-inflammatory mediators (*e.g.*,

cytokines and angiotensin II type 1 receptor) in SMCs (30). In addition, Tangirala *et al.* addressed the importance of macrophage LXR signaling using bone marrow transplantation studies. The advantage of this approach is that only cells derived from bone marrow precursors are LXR null, and that normal LXR function is maintained in liver and intestine. Deletion of LXR from the hematopoetic compartment led to a significant increase in atherosclerotic lesion formation in both apoE–/– (3 fold to 8 fold increase) and LDLR–/– (～3 fold increase) recipient mice. Given that macrophages make up the majority of hematopoetic-derived cells in atherosclerotic lesions, these studies strongly suggest that LXR activity in macrophages is an important determinant of susceptibility to atherosclerosis.

2. Hepatic lipid metabolism in HBV-induced hepatocellular carcinoma

2.1. Clinical significance of hepatitis B virus

Significant differences in the geographic distribution of HCC incidence have led to the identification of chronic hepatitis B virus (HBV) infection as a major risk factor for HCC (33). In recent estimates, 53% of HCC cases worldwide are related to HBV (34). Studies have also estimated that hepatitis B surface antigen (HBsAg) carriers have a 25–37 times increased risk of developing HCC compared to non-infected people (35,36). Other risk factors for HCC include chronic hepatitis C virus infection, exposure to aflatoxin B1, and alcohol abuse. HCC patients have a dismal prognosis, with a 5-year survival rate of 6.5% and a median survival of less than 6 months (37,38).

Although there is compelling evidence that HBV is a major etiologic factor in HCC, the association of chronic HBV infection with HCC remains obscure. Some of the mechanisms that have been suggested for HBV-mediated hepatocarcinogenesis include: persistent inflammation (39,40) and viral integration resulting in chromosomal instability and insertional mutagenesis (41-43); as well as the expression of certain viral proteins such as HBV X protein (HBx) and HBV surface

antigens, which may exert their effects on cell cycle, cell growth, and apoptosis by interfering with cell signaling and transcription (44,45).

The Hepatitis C virus (HCV) is a small (50 nm in size), enveloped, single-stranded, positive sense RNA virus. It is the only known member of the "hepacivirus" genus in the family "Flaviviridae". There are six major genotypes of the hepatitis C virus, which are indicated numerically (e.g., genotype 1, genotype 2, etc.). Replication of HCV involves several steps. The virus replicates mainly in the hepatocytes of the liver, where it is estimated that daily each infected cell produces approximately fifty virions (virus particles) with a calculated total of one trillion virions generated. The virus may also replicate in peripheral blood mononuclear cells, potentially accounting for the high levels of immunological disorders found in chronically infected HCV patients. Hepatitis C virus causes acute and chronic hepatitis (49, 50) an can leads to HCC via oxidative stress, insulin resistance (IR), fibrosis, liver cirrhosis and HCV induced steatosis (51-53). HCV is a major health problem, almost 350 million individuals are chronically HCV infected and 10% of the

Pakistani population is chronically infected with this viral pathogen (50,51). Approximately 40-60% of HCV infected individuals leads to chronic liver disease (52), and prevalence of HCV associated HCC is higher in Pakistan as compare to the rest of world (53).

2.2. Structure and function of Hepatitis B Virus X gene, HBx

HBx gene is the smallest of the four partially overlapping open reading frames of HBV. It comprises 452 nucleotides that encode a 154-amino acid regulatory protein with a molecular mass of 17 kDa (Fig. 2). HBx was the name assigned to the gene and protein because the deduced amino acid sequence did not show homology to any known protein (46,47). It is present in the cytoplasm and, to a lesser extent, the nucleus of hepatocytes. The functions of HBx protein are not fully understood, although it is known to play a regulatory role in HBV replication and is required for the establishment of viral infection (47). The protein is multi-functional. It functions

by protein-protein interaction, and is a promiscuous transactivator of viral and cellular promoters and enhancers. HBx protein does not bind directly to DNA, but causes transcriptional activation by its interaction with nuclear transcription factors and modulation of cytoplasmic signal transduction pathways, including the Ras, Raf, c-jun, MAPK, NF-κB, Jak-Stat, FAK, and protein kinase C pathways, as well as Src-dependent and phosphatiylinositol-3 kinase signaling cascades (44,45). Transcriptional activation is thought to be essential for replication of the virus (46,47). Activation of these signaling pathways may also contribute to HBx protein-mediated hepatocellular carcinogenesis through transactivation of cellular signaling cascades and oncogenes that stimulate proliferation of hepatocytes (48). HBx protein promotes cell cycle progression and inactivates negative growth regulators. In addition, it binds to and inactivates or down-regulates p53 tumor suppressor gene as well as other tumor suppressors and senescence-related factors (42).

2.3. The development of hepatocellular carcinoma by hepatitis virus infection

2.3.1. Evidence for the hepatocarcinogenicity of hepatitis B virus x protein.

Humans, woodchucks, and ground squirrels infected with their respective orthohepadnaviruses, each of which encode the x protein, develop HCC, whereas birds infected with the other members of the Hepadnaviridae, the Avihepadnaviruses, which do not encode the x protein, do not develop the tumor (47). Although HBV DNA integration almost invariably results, to a greater or lesser degree, in loss and rearrangement of viral sequences, the HBx gene is the part of the HBV DNA that is most often included in integrants in the chromosomal DNA of patients with HCC.3 Moreover, integrated HBx gene, even when truncated, often encodes functionally active transactivator proteins and has been shown to express HBx protein (45). HBx protein acts as an oncogene in experimental hepatocellular carcinogenesis. It transforms rodent hepatocytes in vitro and HBx encoding sequences persist in clonally expanding normal and malignant rodent hepatocytes (44-46). In addition, the

protein transforms NIH3T3 cells in co-operation with ras and in transgenic mice without cirrhosis it accelerates the development of HCC in the presence of myc (44,45). HBx protein also increases the susceptibility of these mice to develop HCC when exposed to the carcinogen, diethylnitrosamine (45,46). Moreover, RNA interference (RNAi) markedly reduces HBx mRNA and protein levels and the tumorigenicity of HCC cells that constitutively express HBx protein (54).

2.3.2. Evidence for the hepatocarcinogenicity of hepatitis C virus

Oxidative stress and steatosis is supposed to play a pivotal role in the development of liver injury or HCC in chronic HCV infection (Fig. 3) (51-53). It has been reported that HCV genotype 3a is mostly involved in oxidative stress and HCV induced steatosis, which both contributes in the development of HCC (54-57). Studies have shown the occurrence of oxidation stress and lipid peroxidation in CHC patients leads to HCC . HCC is one of the most common causes of malignancy-related death in Africa and Asia (Koga, 2003). The role of oxidative stress in the progression of

chronic hepatitis and hepatocarcinogenesis is greater in hepatitis C than in other types of hepatitis such as hepatitis B or autoimmune hepatitis. The additive effects of oxidative stress caused by the inflammatory process and that induced by HCV proteins may, furthermore, exert synergistic effects with alterations in intracellular signaling systems such as MAPK, which are also induced by HCV proteins. These synergistic effects may be responsible for rare characteristics, that is, the high incidence and multicentric nature of hepatocarcinogenesis in HCV infection. According to other proposed mechanism HCV Core and NS proteins may accumulate ROS which results in the peroxidation of membrane lipids and structural proteins, which are involved in the trafficking and secretion apparatuses, which block the VLDL secretion and causes mitochondrial dysfunction, DNA and cellular protein damage and further aggravate oxidative stress (57). ROS production causes kupffer cells bursting which results in release of cytokines: TNFα, IL-6 and IL-8 (58). TNFα down regulate the adiponectine thus, inducing IR and steatosis.

2.4. The development of hepatic steatosis by hepatitis virus infection

2.4.1. HBV and heaptic lipogenesis

Abnormal lipid metabolism is also frequently seen in chronic HBV infection; however, very few reports have addressed the steatogenic pathogenesis of HBV infection at a molecular level. A cDNA microarray analysis showed that genes involved in the lipids biosynthesis, such as fatty acid synthase (FAS) and SREBP-2, are upregulated in the HBV-transgenic mouse liver (59). HBx was shown to cause lipid droplet in hepatic cells, mediated by activation of SREBP-1 and peroxisome proliferator activated receptor γ (PPARγ) (60) (Fig. 4). However, the detailed molecular mechanism and in vivo study by which HBV induced events leading to HCC has not been clearly elucidated.

2.4.2. HCV and heaptic lipogenesis

Abnormal hepatic disorder, such as hepatic cellular damage and HCC, impairs

the homeostasis regulating the synthesis and degradation of lipids and lipoproteins (41). HCC lesions at an early stage are often hyperechoic and are composed of well-differentiated cancer cells in triglyceride rich droplets (42,43). Chronic infection with HBV and hepatitis C virus (HCV), two major causes of chronic liver disease, is frequently associated with hepatic lipogenesis. The frequency of hepatic lipogenesis in HCV infection ranges from 31 to 72%, whereas this risk in HBV infection varies from 27 to 51% (49-51). HCV infection-induced hepatic lipogenesis has been well characterized, showing that chronic HCV infection induces histological responses, including the accumulation of lipid droplets and abnormal dysplasia of hepatocytes, activation of insulin resistance, sinusoidal inflammatory cells, dyslipidemia, and HCV genotype 3 (49-51). In experimental animals, abundant HCV replication during acute infection is associated with the modulation of diverse genes involved in lipid metabolism. In addition, drugs that control cholesterol and fatty acid biosynthesis regulate the replication of the subgenomic HCV replicon (52). Among the viral proteins, HCV core protein plays a important role in regulation of the genes related to

fatty acid biosynthesis, including liver X receptor α (LXRα) and sterol regulatory binding protein-1c (SREBP-1c) in the development of hepatic steatosis (53).

3. LXRs in pathophysiology of atherosclerosis

3.1. The role of macrophages in atherosclerosis

Even at very early stages of atherogenesis, many macrophagesand dendritic-like cells have membrane-bound lipid droplets in the cytoplasm. These lipid-loaded cells are called ‘‘foam cells,’’ and their formation begins when phagocytes ingest. The mechanism of this uptake is a widely studied and hotly debated area. Early work suggested that uptake of oxidized LDL occurs via scavenger receptors, notably the type A scavenger receptor (SRA) and a member of the type B family, CD36 (61). However, several gene-targeting studies in apolipoprotein E (ApoE-deficient mice), a widely used model of atherosclerosis in which plasma lipoproteins are elevated due to

absence of the lipoprotein-clearing protein ApoE, indicate that additional mechanisms of foam cell formation are also operational in atherosclerosis (62,63). In vitro work offers plausible mechanisms, including phagocytosis of matrix-retained and aggregated LPs and fluidphase pinocytosis of nonretained native LDL (64,65). Further mechanistic and in vivo studies are needed to fully assess the relative importance of these processes, taking into account stage and location of lesions.

3.2. LXRs and macrophages

Uptake of modified lipids, primarily modified LDL such as oxidized LDL (oxLDL), via scavenger receptors on macrophages is critical to the formation of foam cells. Subsequent accumulation leads to the formation of fatty steaks and ultimately advanced atherosclerotic lesions. It is well established that LXRs antagonize this process by promoting cholesterol efflux via the upregulation of the ABC family transporters resulting in enhanced reverse cholesterol transport (66). Indeed, one would anticipate

that enhanced RCT accounts for much of the anti-atherogenic effects observed with LXR agonists. A important role for the macrophage LXR pathway in atherosclerosis susceptibility was established by Tangirala and colleagues who showed that transplantation of bone marrow lacking LXRα and LXRβ expression into apoE -/- and LDLR -/- recipient mice strongly increased lesion development (67). Moreover, isolated LXRαβ null macrophages displayed increased accumulation of cholesterol. The importance of the LXR pathway in macrophages on the development of atherosclerosis is also supported by work demonstrating that overexpression of LXRα in a macrophage-specific manner in LDLR -/- mice was associated with a reduction in atherosclerosis in the absence of changes in plasma lipid levels (68). Levin and colleagues have further reported that TO901317 had no effect on atherosclerotic lesion development in LDLR -/- mice with bone marrow devoid of LXR, suggesting that most of the atherosclerotic protection afforded by LXR agonists are derived from effects on hematopoeitic cells (69). However, T0901317 was only administered for 6 weeks in this study, and thus one might speculate that other effects may have been seen over a longer treatment period. In

contrast to these studies, Bischoff *et al* reported that LDLR-/- mice transplanted with LXRα-/- LDLR-/- bone marrow exhibit increased en face atherosclerosis, however, this was not as great as the level of atherosclerosis in global LXRα-/- LDLR-/- mice receiving the same bone marrow, suggesting that LXRα deficiency in extra-hematopoietic cells are also involved in the development of atherosclerosis (70). This was further confirmed by studies that restored LXRα expression in hematopoetic cells via BMT into LXRα-/- LDLR-/- mice mice. This manipulation attenuated atherosclerosis but not to the level seen in LDLR-/- mice. These studies raise the possibility that LXRs may exert anti-atherogenic effects on cell types other than macrophages critical to the development of atherosclerotic plaques, perhaps including liver, intestine, endothelial cells and smooth muscle cells.

3.3. Hypoxia and lipid metabolism in atherosclerosis

Atherosclerosis is a chronic and progressive inflammatory disease of the arteries

that is characterized by subendothelial accumulation of lipid-rich macrophages, called foam cells (71,72) (Fig. 5). Although the mechanism has not been clearly established, hypoxic conditions in atherosclerotic lesions contribute to the formation of foam cells (73). Chronic intermittent hypoxia, a condition caused by obstructive sleep apnea, is often associated with atherosclerosis, hyperlipidemia, and a high cardiovascular risk (74). Indeed, an experimental chronic intermittent hypoxia induces atherosclerosis in the presence of diet-induced dyslipidemia in animals (75). The modulation of multiple genes involved in lipid metabolism is associated with hypoxia. Intermittent hypoxia increases mRNA and protein levels of stearoyl-coenzyme A desaturase 1 (SCD-1), an important enzyme in the biosynthesis of triglyceride and phospholipid (74,76). A sterol regulatory element binding protein (SREBP) analog in yeast is upregulated in response to low oxygen, and a similar effect is expected in mammalian cells (77).

RNA interference of hypoxia-inducible factor-1α (HIF-1α), the major transcription regulator of cells exposed to hypoxic conditions, inhibits the formation of macrophage-derived foam cells, and decreases expression of lipogenic genes, such

as the liver X receptor (LXR), adipocyte differentiation-related protein (ADRP) and peroxisome proliferator-activated receptors (PPARs) (78). In a murine model, hypoxia induced an increase in SREBP cleavage-activating protein levels, which was significantly attenuated by partial deficiency of HIF-1α (79). These observations indicate that HIF-1α plays an important role in lipid metabolism and in the formation of lipid-loaded macrophages under hypoxic conditions.

3.4. The paradoxical effect of LXRα in atherosclerosis disease models

LXRα is a nuclear receptor that regulates genes controlling lipid metabolism. LXRα is activated by oxysterols as well as by intermediate products of the cholesterol biosynthetic pathway (80,81). In addition to its well-established role in lipid metabolism, LXRα regulates transcriptional programs involved in the inflammatory response (83). Because LXRα is richly expressed in macrophages in atherosclerotic lesions found in humans, many studies have investigated the LXRα signaling pathway in atherosclerosis using mouse models or primary macrophages

obtained from humans (81–83). It is encouraging that a protective role of LXRα in atherogenesis was evidenced in some of the cardiovascular disease models. Nevertheless, synthetic LXR ligands have been shown to induce lipogenesis and hypertriglyceridemia in mice, raising concerns about the development of these ligands as therapeutic agents against cardiovascular disease (84,85). These paradoxical outcomes from the LXRα activation pathway in atherosclerosis disease models could be a major hurdle for designing strategies using LXR ligands to treat cardiovascular disease (Fig 6).

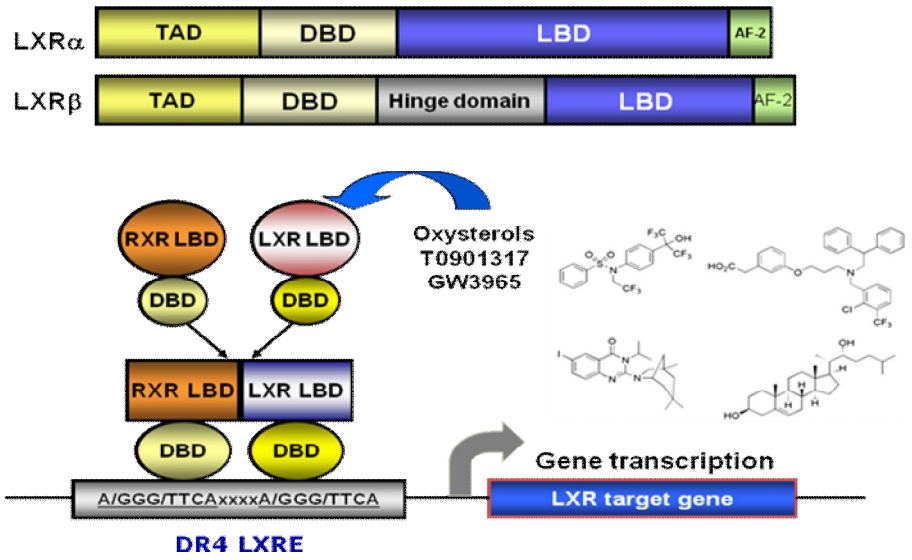

Figure 1. Liver X receptors: LXRα (*Nr1h3*) and LXRβ (*Nr1h2*)

Two LXR subtypes, LXRα and LXRβ, have been identified, that form heterodimers with the 9-cis retinoid X receptor and bind to a specific DNA motif termed the LXR response element (LXRE) (1). LXRE consists of two idealized hexanucleotide sequences (AGGTCA) separated by four bases (DR-4 element).

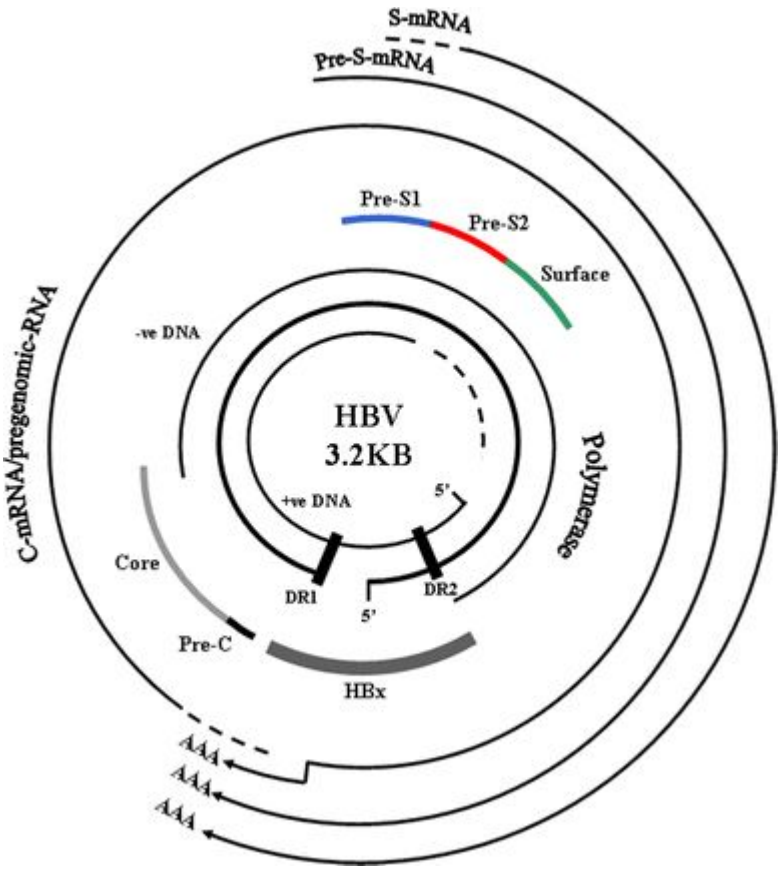

Figure 2. Structure of hepatitis B virus (HBV) genome

The genome of HBV is a double-stranded circular DNA (3.2 kb), which contains four ORF coding for polymerase (P), surface antigens (PreS1, PreS2, and S), precore (PreC), core (C), and X. (Zhang X *et al*., J Lab Clin Med. 2006)

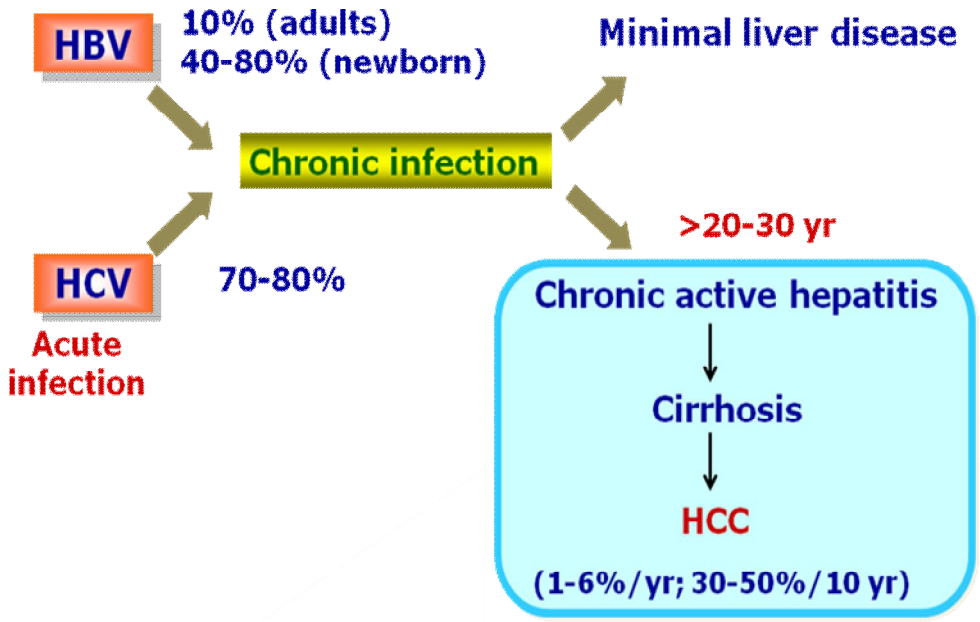

Figure 3. Progression to hepatocarcinoma in HBV- and HCV- infected individuals

Prevalence of cirrhosis and hepatocellular carcinoma resulting from chronic viral hepatitis (HBV and HCV) (48, 49).

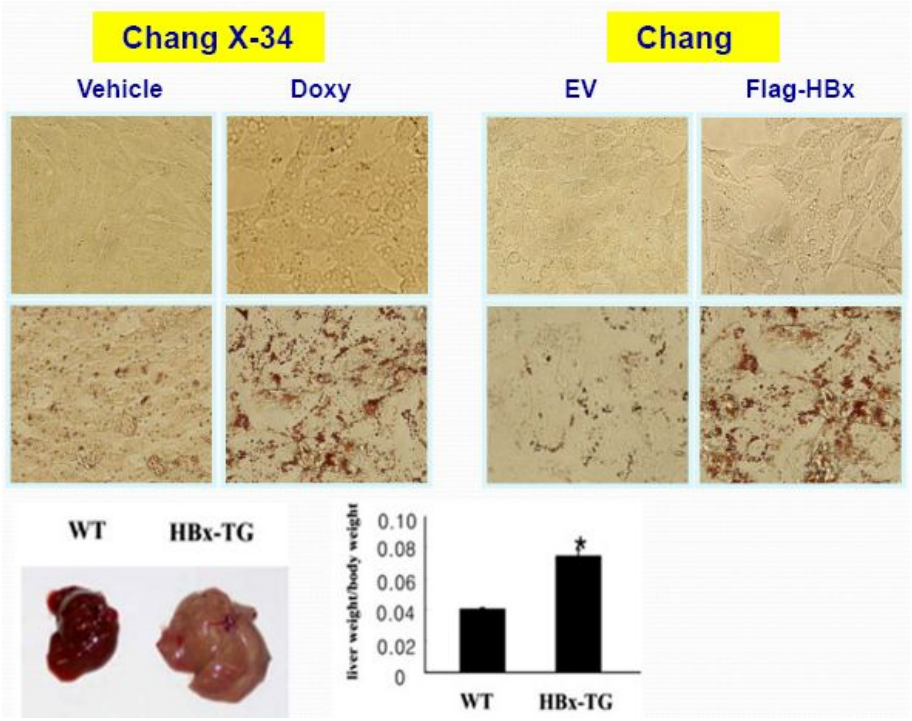

Figure 4. Development of hepatocarcinoma by HBV and HCV

(TOP) Chang were transfected with HBx and Chang X-34 cells cells were treated with 4 μg/ml Doxy for 6 days. At the end of treatment, lipid droplets were stained using Oil-Red O, and photographs were taken. (Bottom) The effect of HBx on hepatic lipid accumulation. Left, macroscopic analysis of livers.. Right, liver weight in HBx transgenic mice and wild-type mice. The liver /body weight ratio was analyzed in wild-type and HBx-transgenic mice at 11 weeks (60).

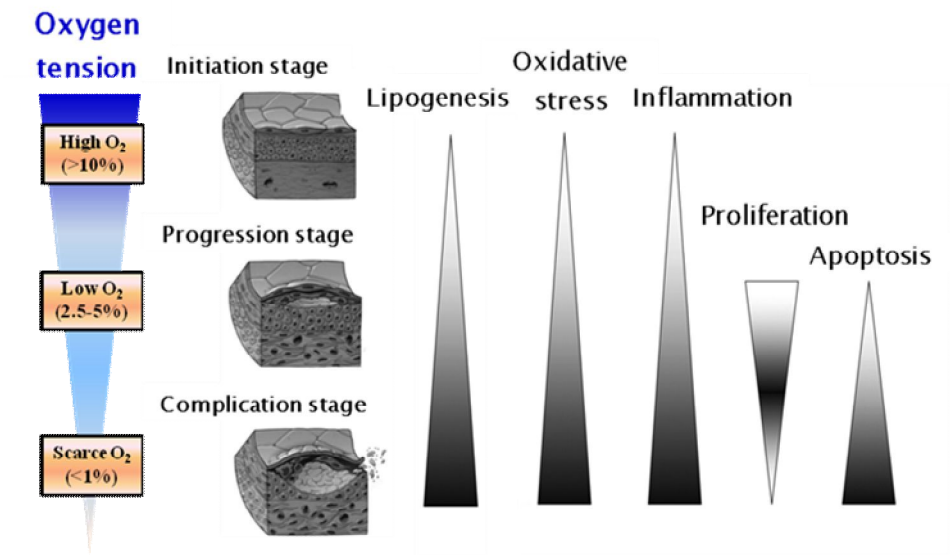

Figure 5. Human atherosclerotic lesions and arterial walls are under hypoxic conditions in vivo and zones of hypoxia occur at depth in this lesion

Hypoxia-induce atherosclerosis. Hypoxia triggers hemodynamic, metabolic, and inflammatory alterations interacting with each other and leading to vascular changes resulting in atherosclerosis (73-75).

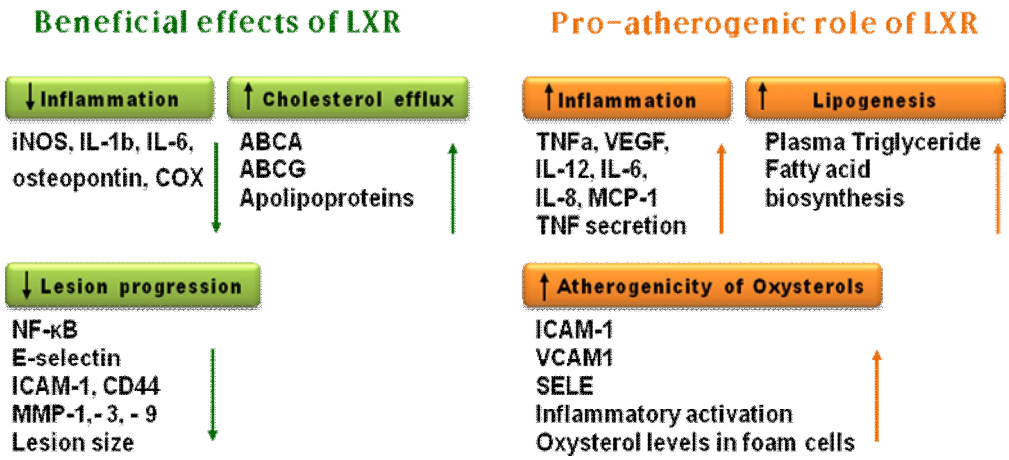

Figure 6. The paradoxical outcomes from the LXR activation pathway in atherosclerosis disease models

The paradoxical outcomes from the LXR activation pathway in atherosclerosis deseases (81–85).

II. PURPOSE OF THIS STUDY

LXRs control the expression of crucial genes associated with cholesterol absorption, excretion and efflux and are therefore key determinants of lipid metabolic disesaes. In addition, many studies have revealed the position of LXRs at the crossroads of lipid metabolism and inflammatory signaling and suggest that these receptors may serve to integrate these pathways in the control of lipid metabolic gene expression.

In the liver, LXRs directly control the expression of SREBP-1, which regulates lipogenic associated enzymes, including FAS. Abnormal lipid metabolism is also frequently seen in chronic HBV infection; however, very few reports have addressed the steatogenic pathogenesis of HBV infection at a molecular level. Several studies have suggested that infection by HBV genotypes B is associated with an increased risk of HCC; however, the molecular mechanism by which HBV induces events leading to HCC has not been clearly elucidated. Also, steatosis has been implicated hepatic fibrosis, hepatitis and liver cancer, its underlying molecular details remains unclear.

Therefore, the purpose of this investigation is to study HBx induced expression of LXR and its lipogenic genes, which may contribute to lipid accumulation. Our focus was on: first, analysis of the expression levels of LXRα and its downstream target genes under HBx. second, analysis of the transactivation function of LXRα by HBx. Third, molecular details on the physical association between LXRα and HBx. Finally, analysis of the correlation LXRα and HBx in HBx-TG mouse and HBV-associated HCC speciments .

Atherosclerosis is a chronic and progressive inflammatory disease of the arteries that is characterized by subendothelial accumulation of lipid-rich macrophages, called foam cells. The liver X receptor (LXR) is an orphan nuclear receptor that functions as a regulator of lipid metabolism in many tissues, however, role of LXRα in the foam cell formation is not known. Although the mechanism is not clearly established, hypoxic conditions in the atherosclerotic lesions contribute to the formation of these lipid-loaded macrophages. Hypoxic regions in atherosclerotic lesions contain large numbers of foam cells, revealing that these cells experience hypoxia during the

development of atherosclerosis. In addition, LXRα is richly expressed in macrophages in atherosclerotic lesions found in humans, many studies have investigated the LXRα signaling pathway in atherosclerosis using mouse models or primary macrophages obtained from humans (81-83). However, the mechanism by which LXR induce events leading to atherosclerosis has not been clearly elucidated. In addition, LXRα protein is expressed in macrophage-lineage foam cells at various stages of atherosclerotic lesions in which hypoxic stress is a prominent feature.

Therefore, the purpose of this investigation is to study a potential cross-talk between HIF-1α and LXRs in macrophages under hypoxia which may contribute to atherosclerotic plaque formation. Our focus was on: First, Analysis of the expression levels of LXRa and its downstream target genes under hypoxic conditions. Second, Analysis of the expression levels of HIF-1α and its target gene VEGF by treatment of TO901317, LXR ligand. Third, Molecular details on the positive cross-talk between HIF-1a and LXRa. Finally, Role of the cross-talk between HIF-1α and LXRα in the cytokine-induced inflammatory response.

III. MATERIALS AND METHODS

1. Molecules and cell-based experiments

1.1. Cells and cell culture

Chang liver, Chang X-34 in which HBx gene expression is under the control of a doxycycline-inducible promoter, and SNU-354 were described previously (86-88). HepG2 was obtained from the American Type Culture Collection. Peripheral blood mononuclear cells (PBMCs) were obtained by ficoll-hypaque density gradient centrifugation from healthy donors. The murine macrophage cell line, RAW 264.7 cells and the human monocytic cell line, THP-1 cells were maintained in Dulbecco's modified eagle's medium containing 10% fetal bovine serum at 37°C in a 5% CO_2/95% air incubator. The cells were exposed to hypoxia (0.1% O2) or treated with TO901317 or 22(*S*)-hydroxycholesterol (HC) (89,90). Desferrioxamine (DFO) or cobalt chloride ($CoCl_2$) were used to induce hypoxia mimicking conditions. Cells were maintained in Dubelco's modified eagle's medium or RPMI containing 10% fetal bovine serum at 37°C in a 5% CO_2/95% air incubator.

1.2. Western blotting, immunoprecipitation and immunocytochemistry

Subcellular fractionation, western blotting, immunoprecipitation and immunocytochemistry were basically performed as previously described using specific antibodies against LXRα (Affinity BioReagents, Golden, CO), LXRα, LXRβ, HBx, HIF-1α, VEGF, SREBP-1c, PPARα, PPARβ, PPARγ, SCD-1, HA, α-actin (Santa Cruz Biotechnology, Santa Cruz, CA), ChREBP (Novus Biologicals, Littleton, CO), FLAG (Sigma, St. Louis, MO) or α-tubulin (Calbiochem, SanDiego, CA) (89-91). Antibodies against FAS were kindly provided by Dr. K-S Kim at Yonsei University College of Medicine.

1.3. Plasmids, transient transfection and reporter gene analysis

The reporters, LXRE-Luc, Gal4-tk-Luc, hypoxia response element (HRE)-tk-Luc, sterol regulatory element (SRE)-Luc, the expression vectors for LXRα and LXRβ, and the truncated pEBG-HIF-1α constructs were as described previously (89-91). The Myc- and the FLAG-tagged HBx were constructed by inserting the HBx cDNA into pCMV-

Myc (Clontech, Palo Alto, CA) and p3XFLAGTM7.1 (Sigma), respectively. The pGAL4-LXRα was constructed by inserting the full-length coding region of human LXRα cDNA into the expression vector containing DNA binding domain (1-147 amino acids) of yeast GAL4. The anti-sense (AS)-LXRα was constructed by inserting the full-length LXRα in reverse orientation into the p3XFLAGTM7.1. All of the new constructs were verified by DNA sequencing. The luciferase reporter encoding the region of the human LXRα promoter, was amplified by PCR and cloned into the pGL3-Basic Vector (92). Transient transfection and reporter gene analysis in RAW 264.7 cells were performed using FuGENE HD Transfection Reagent.

1.4. Transfection of small interfering RNA duplexes

The si-RNA targeting LXRα, LXRβ, HIF-1α, and control non-specific si-RNA (Table I and II) (93) were transfected into cells using FuGENE si-RNA Transfection Reagent.

1.5. Reverse transcriptase-polymerase chain reaction (RT-PCR) and real-time PCR (qRT-PCR)

RT-PCR was performed as described previously with specific primers (Table III and IV) (89). Genes were analyzed under the same conditions used to exponentially amplify the PCR products. qRT-PCR amplifications were performed as previously described (89-91).

1.6. Oil-red O, nile-red staining and lipid analysis

Cells (2 x 10^5 cells per dish) were seeded in 100-mm dishes and incubated overnight. After cells were transfected with si-LXRs and/or treated with doxycycline for 6 days or TO901317 for 3 days, hypoxia for 1 day, the cells were washed twice with PBS and fixed with 10% formalin. Further processes of Oil-Red O or Nile-red staining including fluorescence microscopy and flow cytometry were as previously described (89). Total triglyceride, total cholesterol, HDL, and LDL levels in cell pellet or medium were determined using EnzyChrom Triglyceride or Cholesterol Assay Kit.

1.7. Chromatin immunoprecipitaton (CHIP) assay

HepG2 cells were transfected with 6 μg pCMV-Myc-HBx or empty vector using Welfect-EXTMPLUS (WelGENE Inc., Korea). After 24 h of transfection, cells lysates were obtained and CHIP assay was carried out using specific antibodies as previously described (89). DNA was amplified by PCR using specific primers (sense, 5′-gctcagggtgccagcgaaccagtg-3′ and antisense, 5′-gggttactagcgga cgtccgcc-3′) corresponding to the flanking region of the LXR binding sites on the human SREBP-1c promoter (94). Genomic DNA was amplified by PCR with specific primers corresponding to the flanking region of the HIF-1α binding sites on the mouse promoter of Glut-1 and erythropoietin genes (95).

2. HBx-transgenic mice

The HBx homozygote transgenic mice at different ages and age-matched C57BL/6 wild-type mice were used for this study. The experimental protocol was approved by the

Committee for the Care and Use of Laboratory Animals at Seoul National University, according to the Guide for Animal Experiments edited by Korean Academy for Medical Sciences. Three micrometer section of paraplast-embedded tissue was stained routinely with hematoxylin and eosin (H&E). Oil Red O staining of the frozen liver section was performed as described above. Whole cell lysates obtained from the frozen liver sections were used for western blot analysis.

3. Experiments with clinical samples

3.1. HCC samples, qRT-PCR and immunohistochemistry

Six normal liver samples and thirty patients with HBV-associated HCC were retrospectively identified from the surgical pathology files of the Department of Pathology at Samsung Medical Center. Five patients with normal liver were HBV-negative and HCV-negative and one patient was HBsAg-positive. All samples were collected anonymously according to Institutional Review Board guidelines. All patients had undergone a surgical operation and had received neither chemotherapy nor

radiotherapy before surgical resection. The histopathologic features of HCCs examined were described in Table V. For total RNA extraction from formalin-fixed paraffin-embedded (FFPE) tissues, each tissue section was stained with hematoxylin and non-tumor or cancer regions were microdissected using a laser microdissection system (JungWoo International, Korea) or cut directly with needle from sections. The paradise whole transcript RT reagent system (Arcturus, CA, USA) was used for RNA isolation and RT. Due to the limited amounts of RNA extracted, a half RNA and cDNA was used for RT and qRT-PCR (Table VI), respectively. Hypoxanthine phosphoribosyltransferase 1 was chosen as the endogenous reference gene. All PCR reactions were performed in a Lightcycler 2.0 (Roche Applied Science, Mannheim, Germany) according to standard procedures. PCR efficiency for each gene was determined by measuring serial dilutions of diluted cDNA from HepG2 cells and calculating from Lightcycler 4.0 software. Five HCC specimens showing differential expression of FAS in non-tumor and cancer regions by qRT-PCR were selected for immunohistochemistry. A standard immunohistochemistry was performed using rabbit anti-FAS polyclonal antibody (dilution: 1:50, Santa Cruz Biotechnology) (89).

3.2. Human atherosclerotic specimens and immunohistochemistry

Atherosclerotic plaques were obtained during surgery at Kyungpook national university school of medicine (Daegu, Korea). Serial cryostat sections were prepared, air dried onto microscope slides, and fixed in acetone. This study was approved by the ethics committees of Kyungpook national university school of medicine (Daegu, Korea) in accordance with international guidelines.

3.3. Statistics

Experimental values are expressed as the mean ± S.D. of three independent experiments. The significance of any difference was determined by Student's t tests and expressed as a probability value. For clinicopathological studies, the independent data (normal vs non-tumor region) and the matched data (non-tumor vs cancer) of gene expression was analyzed using Wilcoxon signed rank test and Mann-Whitney test, respectively. Mean differences were considered significant at $P < 0.05$.

Table I: Sequences used for RNA interference (for mouse sample)

si-RNA		Nucleotide sequence
si-LXRα	Sense	5'- cgagcuuugccgugucugutt -3'
	Antisense	5'- acagacacggcaaagcucgtt -3'
si-LXRβ	Sense	5'- gagacaucu cggagguacatt -3'
	Antisense	5'- uguaccuccgagaugucuctt -3'
si-GL3	Sense	5'- guucagcguguccggcgagtt -3'
	Antisense	5'- cucgccggacacgcugaactt -3'
si-GFP	Sense	5'- guucagcguguccggcgagtt -3'
	Antisense	5'- cucgccggacacgcugaactt -3'

Table II: Sequences used for RNA interference
(for mouse sample)

si-RNA		Nucleotide sequence	
si- LXRα	Sense	5'- aggcaugagggaggagugugutt -3'	
	Antisense	5'- acacacuccucccucaugccutt -3'	
si-LXRβ	Sense	5'- gagacaucucggagguacatt -3'	
	Antisense	5'- uguaccuccgagaugucuctt -3'	
si-HIF-1α	Sense	5'- agatgagttctgaacgtcgtt -3'	
	Antisense	5'- cgacgttcagaactcatcttt -3'	
si-Control (GL3)	Sense	5'- cuuacgcugaguacuucgatt -3'	Figure 13 and 14
	Antisense	5'- ucgaaguacucagcguaagtt -3'	
si-Control (GFP)	Sense	5'- guucagcguguccggcgagtt -3'	Figure 19 and 20
	Antisense	5'- cucgccggacacgcugaactt -3'	

Table III: Primer sequences used for RT-PCR and qRT-PCR (for human sample)

Gene	Accession number		Nucleotide sequence	Annealing Temperature	
LXRα	NM_ 005693	Sense	5'- agtgtcggcttcgcaaat -3'	57℃	RT-PCR & qRT-PCR
		Antisense	5'- agaagcatcacctcgatcg -3'		
LXRβ	NM_ 007121	Sense	5'- gagtcacagtcacagtcgcag -3'	58℃	RT-PCR
		Antisense	5'- tctctagcagcatgatctcgat -3'		
		Sense	5'- acagcaaggacgacttccac -3'	58℃	qRT-PCR
		Antisense	5'- actcgaagatggggttgatg -3'		
PPARα	NM_001001928	Sense	5'- atcggcgaggatagttct -3'	58℃	RT-PCR
		Antisense	5'- aatcgcgttgtgacat -3'		
		Sense	5'- gcactggaactggatgacag -3'	58℃	qRT-PCR
		Antisense	5'- tttagaaggccaggacgatct -3'		
PPARβ	NM_006238	Sense	5'- cagaagaagaaccgcaaca -3'	58℃	RT-PCR & qRT-PCR
		Antisense	5'- cgccatacttgagaagggt -3'		
PPARγ	NM_138711	Sense	5'- cagatccagtggttgcag -3'	59℃	RT-PCR
		Antisense	5'- gtgagcggactctggatt -3'		
		Sense	5'- caggaaagacaacagacaaatca -3'	58℃	qRT-PCR
		Antisense	5'- ggggtgatgtgtttgaacttg -3'		
FAS	NM_004104	Sense	5'- tgctaggtatggagttctcgg -3'	58℃	RT-PCR
		Antisense	5'- tggttctgagaaaggtcgaatt -3'		
		Sense	5'- tacggctccacgctcttc -3'	58℃	qRT-PCR
		Antisense	5'- gagtcttcgtcagccaggat -3'		
SREBF	NM_001005291	Sense	5'- gcttcagcttatcaacaacc -3'	58℃	RT-PCR
		Antisense	5'- cttcctgtagagaagcctcc -3'		
SCD-1	NM_005063	Sense	5'- actggtgatgttccagagga -3'	58℃	RT-PCR
		Antisense	5'- gtttccatctccggttcttt -3'		

ChREBP	BC012925	Sense	5'- acagcaacaagaccgagaac -3'	58℃	RT-PCR
		Antisense	5'- tgaaggactcaaacagaggc -3'		
β-actin	X03672	Sense	5'- cgtgggccgccctaggcacca -3'	55℃	RT-PCR & qRT-PCR
		Antisense	5'- ttggcttagggttcaggggg -3'		

Table IV: Primer sequences used for RT-PCR and qRT-PCR (for mouse sample)

Gene	Accession number		Nucleotide sequence	Annealing Temperature	
LXRα	NM 005693	Sense	5'- agtgtcggcttcgcaaat -3'	57℃	RT-PCR
		Antisense	5'- agaagcatcacctcgatcg -3'	human	
	NM 013839	Sense	5'- tgaagaaactgaagcggcaa -3'	58℃	qRT-PCR
		Antisense	5'- ttgcagcctctctacttgga -3'	mouse	RT-PCR
LXRβ	NM 009473	Sense	5'- ctagccatcatctcggtcca-3'	57℃	qRT-PCR
		Antisense	5'- gtccatcttcaagaagacacca -3'	mouse	RT-PCR
FAS	NM007988	Sense	5'- cttgccactgtagtacaagca -3'	58℃	qRT-PCR
		Antisense	5'- aggtcctttccaggaatgga -3'	mouse	RT-PCR
SREBP-1c	NM011480	Sense	5'- agttctcagatgcccttgga -3'	59℃	qRT-PCR
		Antisense	5'- tcatgtaggaataccctcctc -3'	mouse	RT-PCR
SCD-1	NM009127	Sense	5'- tctccagttcttacacgacca -3'	59℃	RT-PCR
		Antisense	5'- gcttgtagtacctcctctgga -3'	mouse	
ADRP	NM007408	Sense	5'- attgcggttgccaataccta-3'	58℃	RT-PCR
		Antisense	5'- cgagacatagagcttatcctga -3'	mouse	
CD36	NM001001548	Sense	5'- cgtgggccgccctaggcacca -3'	55℃	RT-PCR
		Antisense	5'- ttggcttagggttcaggggg -3'	human	
	NM001159558	Sense	5'- cgtgggccgccctaggcacca -3'	55℃	RT-PCR
		Antisense	5'- ttggcttagggttcaggggg -3'	mouse	
ABCA1	NM001001548	Sense	5'- cgtgggccgccctaggcacca -3'	55℃	RT-PCR
		Antisense	5'- ttggcttagggttcaggggg -3'	human	
	NM001159558	Sense	5'- cgtgggccgccctaggcacca -3'	57℃	RT-PCR
		Antisense	5'- ttggcttagggttcaggggg -3'	mouse	
HIF-1α	NM181054	Sense	5'- ccccagattcaggatcagaca -3'	58℃	qRT-PCR
		Antisense	5'- ccatcatgttccatttttcgc -3'	human/mouse	RT-PCR

VEGF	NM001025370	Sense	5'- ctgctgtcttgggtgcattgg -3'	58℃	qRT-PCR
		Antisense	5'- caccgcctcggcttgtcacat -3'	human/mouse	RT-PCR
β-actin	X03672	Sense	5'- cgtgggccgccctaggcacca -3'	55℃	qRT-PCR
		Antisense	5'- ttggcttagggttcaggggggg -3'	human/mouse	RT-PCR

Table V: Clinicopathologic parameters of 30 HCC patients

Case No.	Histo-logical Grade[1]	HBV[2]	Age	Sex	Tumor Size (mm)	Tumor Capsule	Micro-vascular invasion[3]	Major portal vein invasion	Intra-hepatic metastasis[4]	Tumor stage[5]	Non-Tumor Region[6]
1	1	+	53	M	24	-	-	-	-	I	FAT
2*	1	+	66	M	28	+	-	-	-	I	CPH
3	1	+	64	M	12	+	-	-	-	I	CPH
4	1	+	58	M	25	+	-	-	-	I	CIR
5	1	+	56	M	12	+	-	-	-	I	CIR
6	1	+	56	M	25	+	-	-	-	I	CIR
7	1	+	45	M	32	+	-	-	-	I	CIR
8	1	+	63	M	53	+	-	-	-	I	CPH
9*	1	+	66	M	27	+	+	-	-	II	CIR
10	1	+	50	M	47	+	-	-	-	I	CPH
11	2	+	38	M	80	+	+	-	-	II	CAH
12	2	+	40	M	59	-	+	-	-	II	CAH
13	2	+	59	M	35	-	+	-	-	II	CAH
14	2	+	58	M	80	+	+	-	-	II	CAH
15	2	+	41	M	80	-	+	-	-	II	CAH
16	2	+	46	M	15	-	+	-	-	II	CIR
17	2	+	37	M	70	-	+	-	-	II	CPH
18*	2	+	58	M	44	+	+	-	-	II	CIR
19*	2	+	60	F	31	+	-	-	-	I	CIR
20	2	+	40	M	90	-	+	-	-	II	CAH

21	3	+	30	M	70	-	+	+	+	III	CIR
22	3	+	48	M	110	-	+	-	+	II	CPH
23	3	+	60	M	80	-	+	-	-	II	NON
24	3	+	42	M	55	-	+	-	+	II	CIR
25	3	+	43	M	50	+	+	-	+	II	CIR
26	3	+	48	M	68	+	+	-	-	IV	CIR
27	3	+	40	M	65	+	+	-	-	II	CAH
28	3	+	45	M	100	-	+	-	+	II	CPH
29*	3	+	42	M	55	+	+	-	-	II	CIR
30	3	+	31	F	70	-	+	-	+	II	CPH

[1] Edmondson-Steiner's grade

[2] HBsAg-positive and anti-HBs Ab-negative

[3] Microvascular invasion was considered as present when at least one or more endothelial cells or the tunica media of the vessel were recognized to surround a neoplastic cell group.

[4] Intrahepatic metastasis and tumor capsule formation were matched to the criteria of the Liver Cancer Study Group of Japan.

[5] The tumor stage was determined according to the AJCC cancer staging criteria.

[6] FAT: Fatty Change, CPH: Chronic Persistent Hepatitis, CAH: Chronic active hepatitis, CIR: Cirrhosis

* Five cases selected for FAS IHC.

Table VI: qRT-PCR primers and taqman probes used for clinical specimen analysis

Gene	Accession number	Probe (UPL Probe No.)	Nucleotide sequence		Annealing Temperature	PCR efficiency (dilution)[1]
LXRα	NM_005693	5	Sense	5'- cagggctccagaaagagatg -3'	55℃	1.953
			Antisense	5'- acagctccaccgcagagt -3'		
LXRβ	NM_007121	85	Sense	5'- ccgctgttgcttggagag -3'	55℃	1.894
			Antisense	5'- atccagggaactcgtggtag -3'		
FAS	NM_004104	11	Sense	5'- caggcacacacgatggac -3'	55℃	2.03
			Antisense	5'- cggagtgaatctgggttgat -3'		
SREBF	NM_001005291	77	Sense	5'- gctcctccatcaatgacaaaa -3'	55℃	1.914
			Antisense	5'- tgcgcaagacagcagattta -3'		
SCD-1	NM_005063	82	Sense	5'- cctagaagctgagaaactggtga -3'	55℃	1.894
			Antisense	5'- acatcatcagcaagccaggt -3'		
HPRT1	NM_000194	Specific Probe[2]	Sense	5'- ctcaactttaactggaaagaatgtc -3'	55℃	1.904
			Antisense	5'- tccttttcaccagcaagct - 3'		

[1] PCR efficiency for each gene was determined by using serial dilutions of cDNA from HepG2 cells for PCR and then calculating the efficiency using the Roche Lightcycler software 4.0

[2] DYXL-ttgctttccttggtcaggcagtataatc-BHQ2

IV. RESULTS

1. Roles of LXRs in HBx-induced lipogenesis in HBV-associated HCC

1.1. HBx induces expression and transcriptional activity of LXR

The observation that hepatic steatosis frequently occurs in HBx-transgenic mice attributes a critical role to HBx in steatosis. Interestingly, HBx may trigger LXR-mediated lipogenic signaling, since LXRα and LXRβ are the major regulators of hepatic lipid accumulation via the modulation of the expression of lipogenic genes, such as SREBP-1c, FAS, SCD-1 and ChREBP (96,97). The expression of LXRα and LXRβ was altered by HBx in the Chang X-34 cell line, in which the expression of HBx is under control of an inducible doxycycline promoter. HBx expression-induced by doxycycline treatment, profoundly augmented the expression of LXRα, LXRβ, and their downstream target genes, both at the protein and mRNA levels (Fig. 7A and B). Similar results were obtained when HBx was exogenously introduced in Chang cells by transient transfection of the vector encoding HBx cDNA (Fig. 7A and B). In order to determine whether the HBx-induced LXRα was transcriptionally active, it

was carried out reporter gene analysis in Chang X-34 cells using a reporter gene containing LXRE sequences (89). Doxycycline induced the reporter activity in a dose-dependent manner, which was further enhanced by addition of a LXR ligand, TO901317 (Fig. 7C). At the same time, a similar observation was reported (98).

1.2. LXR mediates HBx-induced lipogenesis in liver cells

Next, it was carried out an RNA interference experiment to examine whether the induction of LXR played a role in HBx-induced lipogenic gene expression and lipogenesis. Transfection of either si-LXRα or si-LXRβ largely decreased the levels of LXR lipogenic target genes such as SREBP-1c and FAS proteins (Fig. 8A). When the expression of LXRα was decreased by AS-LXRα, HBx-induced PPAR expression was significantly decreased (Fig. 8B). Consistently, the reporter gene containing LXRE or SRE that was activated by doxycycline and TO901317 was dramatically repressed by si-LXRα (Fig. 8C). Importantly, transfection of si-LXRα and si-LXRβ largely blocked the lipid droplet accumulation induced by doxycycline

treatment in Chang X-34 cells when examined by microscopy or FACS analysis (Fig. 8 D,E).

1.3. HBx interacts with LXRα

To determine cross talk between LXRα and HBx , it examined whether these proteins were physically associated. Firstly, immunofluorescence study was carried out using endogenous HBx expression cell line, SNU-354 cells in which HBV genome is integrated. HBx was expressed both in the cytoplasm and the nucleus while LXRα was predominantly expressed in the nucleus. The expression of HBx in the nucleus was overlayed with that of LXRα (Fig. 9A). Results from the subcellular fractionation further support this observation. When HBx was exogenously introduced in HepG2 cells, HBx was mainly expressed in the nucleus and it induced the nuclear expression of LXRα (Fig. 9B). Secondly, LXRα and HBx reciprocally coimmunoprecipitated, indicating that these factors physically interact (Fig. 9C).

1.4. HBx increases transactivation function of LXRα

Next, it was carried out whether HBx enhance the transactivation function of LXRα using a Gal4-driven luciferase reporter system (91). TO901317 and doxycycline enhanced the Gal4-LXRα-induced reporter activity by about 8- and 2-fold, respectively. Doxycycline together with TO901317 synergistically activated the reporter. Similar results were obtained when HBx was transiently expressed in Chang cells (Fig. 10A). Consistent with this result, CHIP assay showed that LXRα and the coactivator CREB binding protein (CBP) were able to bind to the LXRE of SREBP-1c promoter in the presence of HBx (Fig. 10B). Together, these results suggest that HBx interacts with LXRα and that this interaction may increase the transactivation function of LXRα by recruiting CBP onto the promoter of the LXR target genes.

1.5. Increases in expression level of LXR in liver samples of HBx-expressing transgenic mice

Next it was examined the expression of LXRα in liver samples obtained from HBx-transgenic mice. Consistently with previous observations, lipid droplet enhanced

in the liver sections from the HBx-transgenic mice (Fig. 11A). Expression of LXRα and LXRβ was strongly expressed in the HBx TG livers to compare with wild type tissues. Similarly, the expression of SREBP-1c, FAS, SCD-1, and ChREBP was dramatically elevated in the HBx TG liver, indicating a strong correlation between the activation of LXRs and HBx expression (Fig. 11B).

1.6. Enhances in expression level of LXRβ and target genes in liver tissues of HCC patients

Finally, the expression levels of LXR, SREBP-1c, FAS, and SCD-1 in 30 HBV-associated HCC specimens was assessed using qRT-PCR after microdissection of the HCC tissues and the adjacent non-tumorous tissues (Table V). The expression level of LXRβ was significantly increased ($P = 0.036$) in the HCC cells, when compared with expression in the adjacent non-tumorous region. However, the expression level of LXRα was not significantly different (Fig. 12A). Consistently, the expression levels of SREBP-1c, FAS, and SCD-1 were significantly increased in the HCC tissues (SREBP-1c, $P = 0.008$; FAS and SCD-1, $P = 0.001$). Most strikingly, the induction of

FAS and SCD-1 was greater than two-fold in about 50% of the HCC samples. A strong immunoreactivity for FAS in cancerous lesions was observed in all five HCC samples showing a strong mRNA induction of FAS by qRT-PCR (Table VI, Fig. 12B). The results obtained from the HBx-transgenic mice and clinicophathological studies strongly support our hypothesis that HBx activates LXR and its downstream genes, and that this may contribute to the development of HBV-associated HCC.

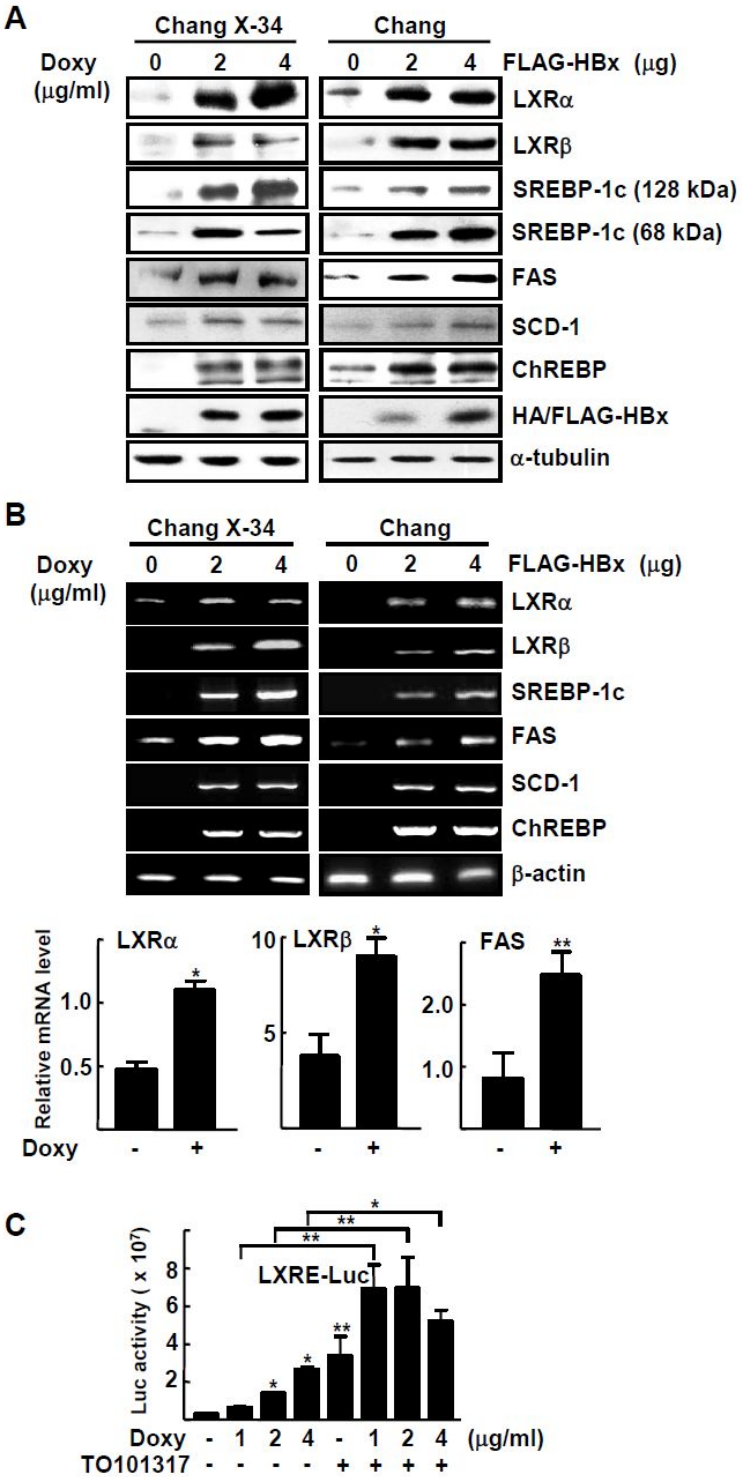
A
Chang X-34
Chang
Doxy (μg/ml)
0 2 4 0 2 4
FLAG-HBx (μg)
LXRα
LXRβ
SREBP-1c (128 kDa)
SREBP-1c (68 kDa)
FAS
SCD-1
ChREBP
HA/FLAG-HBx
α-tubulin
B
Chang X-34
Chang
Doxy (μg/ml)
0 2 4 0 2 4
FLAG-HBx (μg)
LXRα
LXRβ
SREBP-1c
FAS
SCD-1
ChREBP
β-actin
Relative mRNA level
LXRα
LXRβ
FAS
Doxy - + - + - +
C
Luc activity (x 10⁷)
LXRE-Luc
Doxy - 1 2 4 - 1 2 4 (μg/ml)
TO101317 - - - - + + + +

Figure 7. HBx increases expression of LXRα and LXRβ and their downstream target genes. (A) Chang X-34 cells were treated with doxycycline (Doxy) or vehicle for 24 h. Chang cells were transfected with p3XFLAG7.1-HBx. Expression of proteins was analyzed by western blotting. **(B)** Total RNA was prepared and analyzed for transcripts by RT-PCR (upper) and real-time PCR (lower). *$P < .05$, **$P < .01$ (n=3) vs control **(C)** Chang X-34 cells were transfected with 0.1 μg LXRE-Luc, and transfected cells were incubated with 2 μg/ml Doxy and/or 1 μM TO901317 for 24 h. *$P < .05$, **$P < .01$ (n=3)

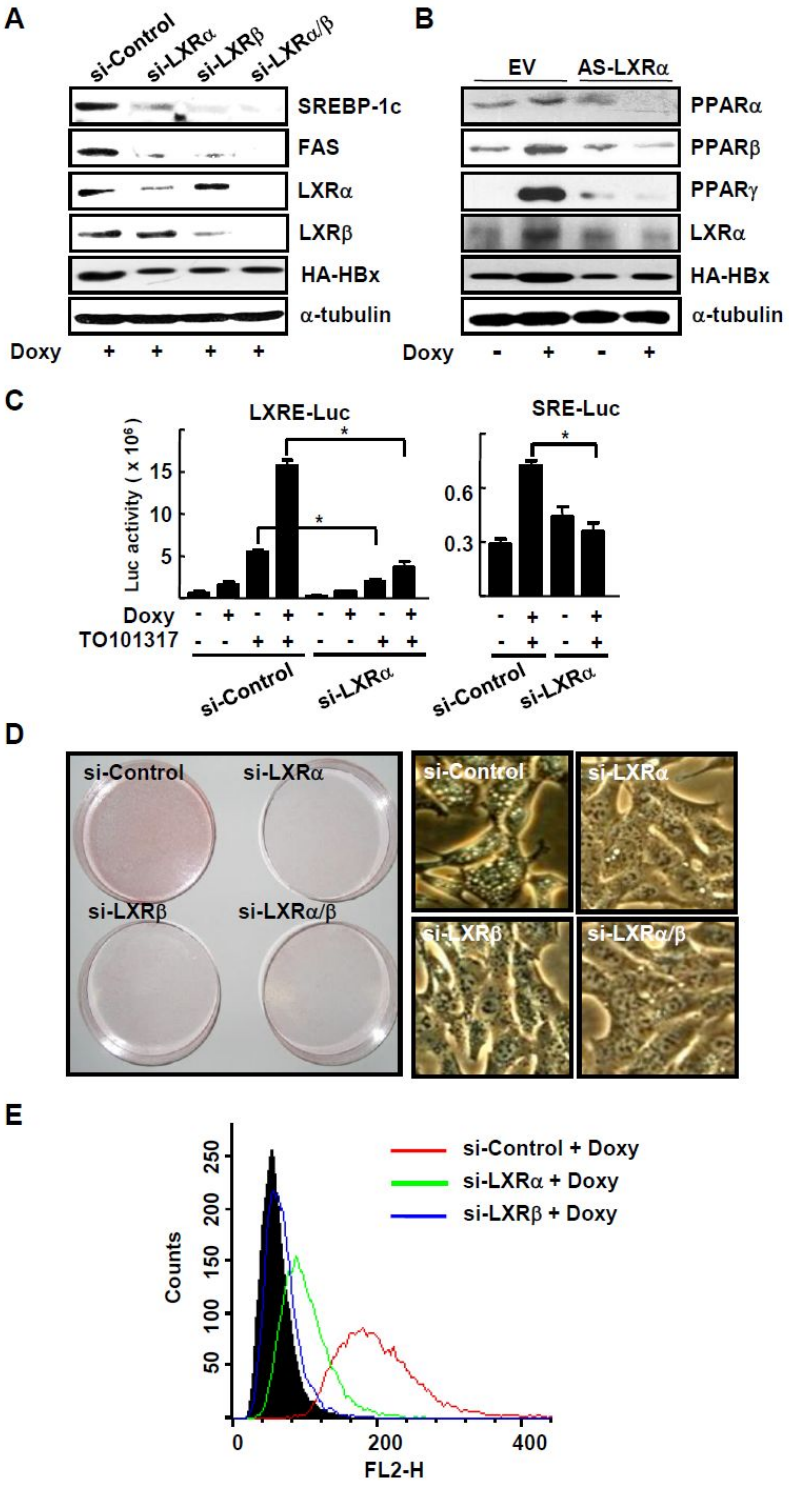
A
si-Control
si-LXRα
si-LXRβ
si-LXRα/β
SREBP-1c
FAS
LXRα
LXRβ
HA-HBx
α-tubulin
Doxy + + + +
B
EV
AS-LXRα
PPARα
PPARβ
PPARγ
LXRα
HA-HBx
α-tubulin
Doxy - + - +
C
LXRE-Luc
SRE-Luc
Luc activity (x 10⁶)
15
10
5
0.6
0.3
Doxy
TO101317
si-Control
si-LXRα
D
si-Control
si-LXRα
si-LXRβ
si-LXRα/β
E
si-Control + Doxy
si-LXRα + Doxy
si-LXRβ + Doxy
Counts
50 100 150 200 250
0 200 400
FL2-H

Figure 8. LXRα mediates HBx-induced lipogenesis. (A) Chang X-34 cells were transfected with si-control or si-LXR as indicated. **(B)** Chang X-34 cells were transfected with empty vector (EV) or AS-LXRα. Transfected cells were treated with 2 μg/ml Doxy for 24 h. Whole cell lysates were analyzed by western blotting. **(C)** Chang X-34 cells were co-transfected with 0.1 μg LXRE-Luc or 10 ng SRE-Luc together with si-control or si-LXRα. Transfected cells were incubated with 2 μg/ml Doxy and/or 1 μM TO901317 for 24 h as indicated. **P* < 0.05 (n=3) **(D)** Chang X-34 cells were transfected with si-control or si-LXR and transfected cells were treated with 4 μg/ml Doxy for 6 days. At the end of treatment, lipid droplets were stained using Oil-Red O, and photographs were taken. **(E)** Chang X-34 cells were treated as (D) and flow cytometry was performed after staining with Nile red. The histogram for si-control transfection with vehicle treatment was filled with black.

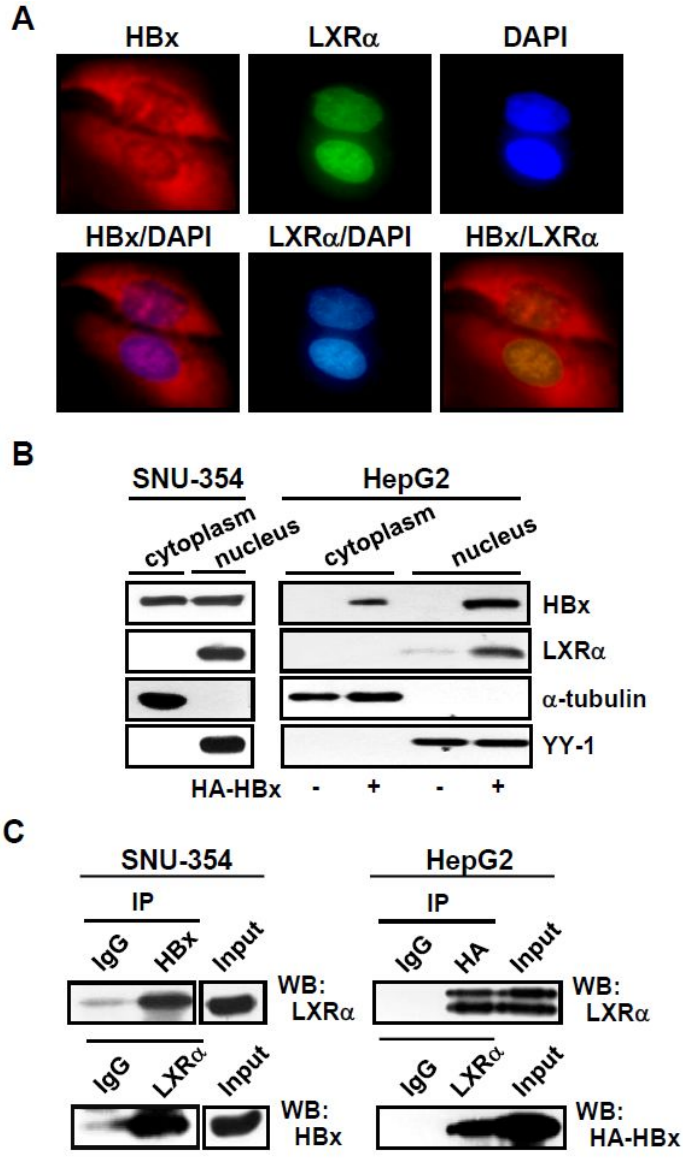
A
HBx
LXRα
DAPI
HBx/DAPI
LXRα/DAPI
HBx/LXRα
B
SNU-354
HepG2
cytoplasm
nucleus
cytoplasm
nucleus
HBx
LXRα
α-tubulin
YY-1
HA-HBx - + - +
C
SNU-354
HepG2
IP
IP
IgG
HBx
Input
IgG
HA
Input
WB: LXRα
WB: LXRα
IgG
LXRα
Input
IgG
LXRα
Input
WB: HBx
WB: HA-HBx

Figure 9. HBx interacts with LXRα in the nucleus. (A) SNU-354 cells were fixed and expression of HBx and LXRα was visualized by immunocytochemistry using specific antibodies. 4,6-diaminidino-2-phenylindole was used to stain the nuclei. **(B)** Cytoplasmic and nuclear fractions were obtained from SNU-354 cells or HepG2 cells that were transfected with pCMV-HA-HBx or empty vector. Expression of the indicated proteins was analyzed by western blotting. (C) Whole cell lysates were prepared from SNU-354 cells or HepG2 cells that were transfected with pCMV-HA-HBx. Immunoprecipitation (IP) was performed using the indicated antibodies, and the resulting precipitates were analyzed by western blotting (WB).

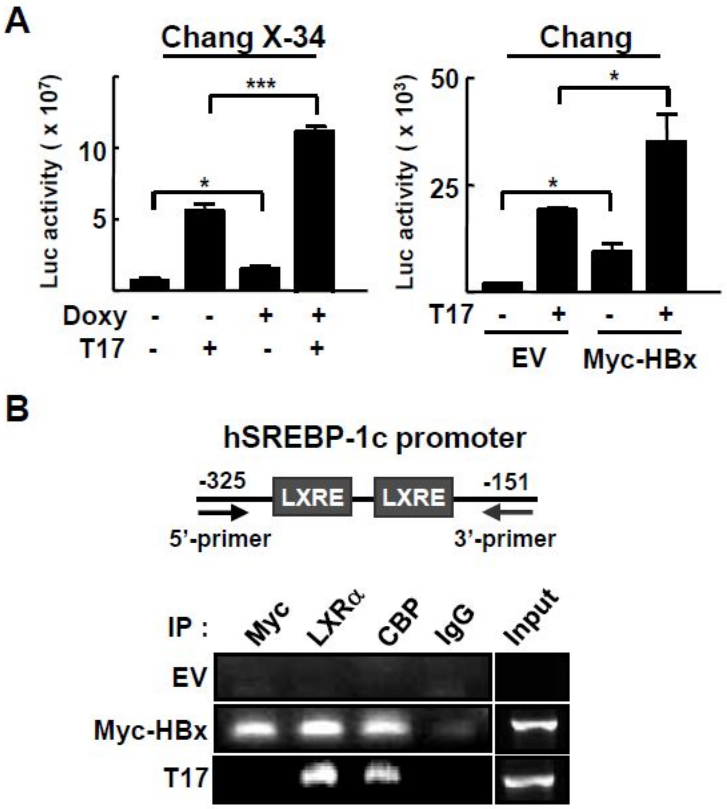
A
Chang X-34
Chang
Luc activity (x 10⁷)
Luc activity (x 10³)
***
*
*
*
10
5
50
25
Doxy - - + +
T17 - + - +
T17 - + - +
EV
Myc-HBx
B
hSREBP-1c promoter
-325
LXRE
LXRE
-151
5'-primer
3'-primer
IP :
Myc
LXRα
CBP
IgG
Input
EV
Myc-HBx
T17

Figure 10. HBx enhances transactivation function of LXRα. (A) Chang X-34 cells were transfected with Gal4-tk-Luc and pGal4-LXRα. Chang cells were transfected with Gal4-tk-Luc and pGal4-LXR together with empty vector (EV) or pCMV-Myc-HBx. Transfected cells were treated with 2 μg/ml doxycycline (Doxy) and/or 1 μM TO901317 (T17) for 24 h. * $P < 0.05$, *** $P < 0.001$ (n=3) **(B)** Schematic presentation for CHIP assay (upper). HepG2 cells were transfected with EV or pCMV-Myc-HBx. DNA fragments that were immunoprecipitated (IP) using the indicated antibodies were amplified by PCR (lower).

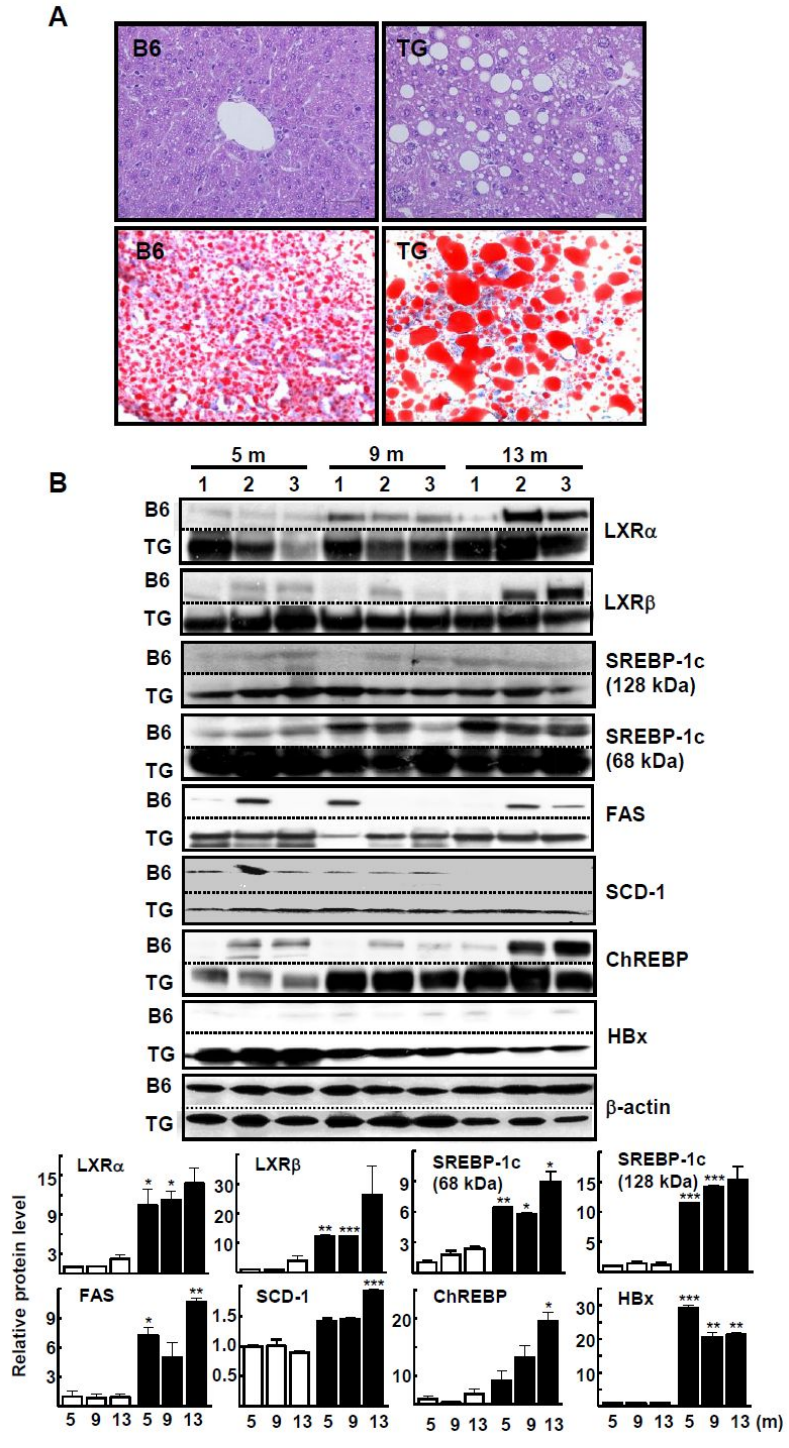
A
B6
TG
B6
TG
B
5 m
9 m
13 m
1 2 3 1 2 3 1 2 3
B6
TG
LXRα
LXRβ
SREBP-1c (128 kDa)
SREBP-1c (68 kDa)
FAS
SCD-1
ChREBP
HBx
β-actin
Relative protein level
LXRα
LXRβ
SREBP-1c (68 kDa)
SREBP-1c (128 kDa)
FAS
SCD-1
ChREBP
HBx
5 9 13 5 9 13 (m)

Figure 11. Increases in expression level of LXRs and its downstream target genes in the liver of HBx-transgenic mice. (A) H&E staining (upper) and Oil-Red O staining (lower) of the liver sections from 9 month-old HBx-TG and aged-matched C57BL/6 wild type mice (B6). **(B)** Whole cell lysates were obtained from the liver of the indicated aged B6 and HBx-TG mice, and were analyzed for protein levels by western blotting (upper). Density of each protein band was determined using an image analysis system and normalized to that of the corresponding α-tubulin. Y-axis represents the relative protein level to compare with that of 5 month-old WT mice. *$P < 0.05$, ** $P < 0.005$, *** $P < 0.0001$ *vs* age-matched B6 mice (n=3) (lower).

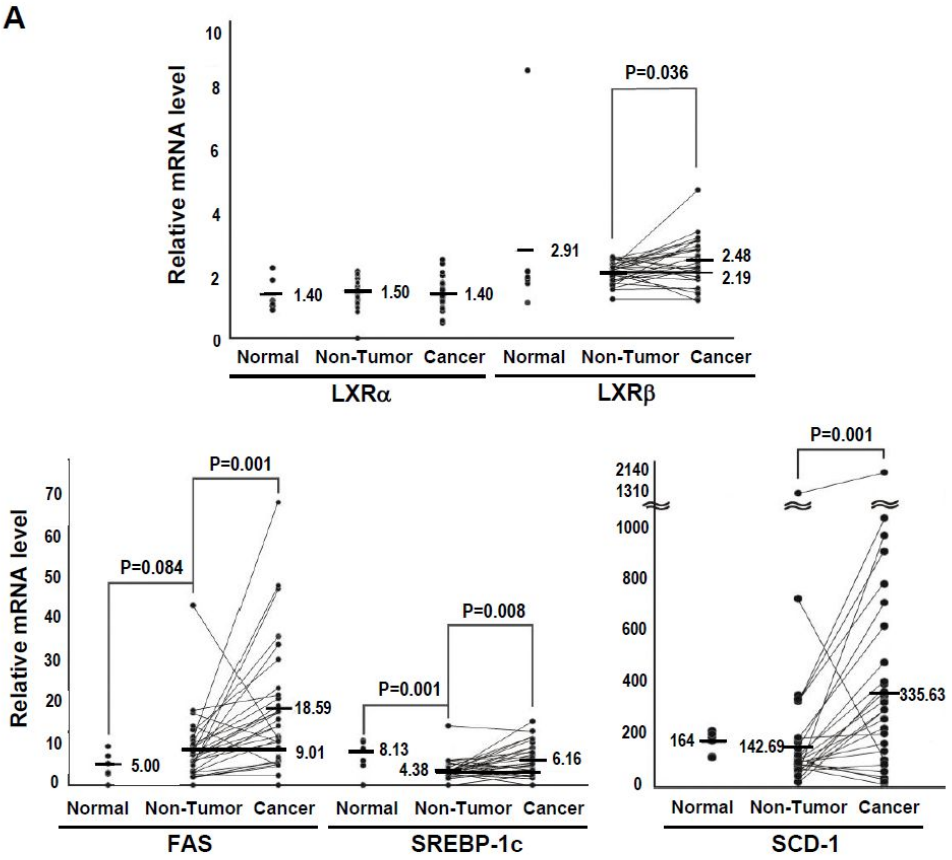
A
Relative mRNA level
10
8
6
4
2
0
P=0.036
1.40
1.50
1.40
2.91
2.48
2.19
Normal
Non-Tumor
Cancer
Normal
Non-Tumor
Cancer
LXRα
LXRβ
Relative mRNA level
70
60
50
40
30
20
10
0
P=0.001
P=0.084
P=0.008
P=0.001
18.59
9.01
5.00
8.13
4.38
6.16
Normal
Non-Tumor
Cancer
Normal
Non-Tumor
Cancer
FAS
SREBP-1c
2140
1310
1000
800
600
400
200
0
P=0.001
335.63
164
142.69
Normal
Non-Tumor
Cancer
SCD-1

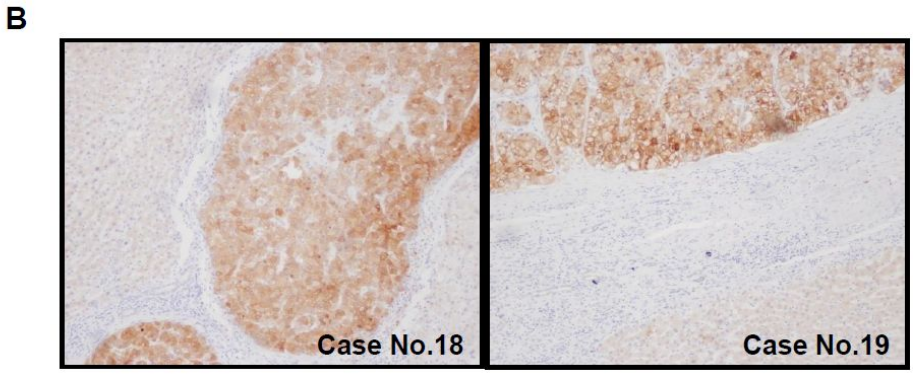
B
Case No.18
Case No.19

Figure 12. Increases in LXRβ, SREBP-1c, FAS, and SCD-1 expression in HBV-associated HCC. (A) The HBV-associated HCC tissues were obtained from 30 HCC patients. qRT-PCR was performed with cDNA prepared with total RNA isolated from the microdissected non-tumor or cancer regions. The independent data (normal vs non-tumor region) and the matched data (non-tumor vs cancer) of gene expression was analyzed using Wilcoxon signed rank test and Mann-Whitney test, respectively. **(B)** Immunohistochemical staining of FAS in adjacent non-tumor and in cancerous regions obtained from the indicated Cases. Original magnification, X100.

2. Roles of LXRs in hypoxia-induced foam cell formation in atherosclerotic lesion

2.1. Expression of LXRα and its downstream target genes increases under hypoxia

The LXRα protein is expressed in macrophage-lineage foam cells at various stages of atherosclerotic lesions in which hypoxic stress is a prominent feature (82). Therefore, it was hypothesized that cross-talk between HIF-1α and LXRα may occur in macrophages under hypoxia, which may contribute to atherosclerotic plaque formation. Therefore, first it was examined whether expression of LXRα and its downstream target genes was influenced under hypoxic conditions. Primary human macrophages obtained from healthy donors and murine RAW 264.7 cells were cultured under hypoxia. Protein levels of LXRα and its downstream target genes, SREBP-1c and fatty acid synthase (FAS), increased under hypoxia, which was similar to the induction of HIF-1α and VEGF under the same conditions (Fig. 13A).

Knockdown of HIF-1α using si-RNA completely abolished the induction of LXRα, SREBP-1 and FAS, indicating that the induction of LXRα was HIF-1α-dependent. Interestingly, knockdown of LXRα also blocked the induction of HIF-1α, further suggesting the existence of cross-talk between hypoxia and LXRα signaling (Fig. 13B). The induction of LXRα was confirmed by LXRE-tk-Luc reporter gene analysis. Treatment with DFO, a hypoxia-mimicking reagent, significantly induced the reporter activity, which was further enhanced by the addition of the synthetic LXR ligand, TO901317 (Fig. 13C). Hypoxia led to significant upregulation of LXRα and its downstream target genes at the mRNA level (Fig. 13D). A reporter encoding the 5′ upstream promoter of the human LXRα gene was activated in the presence of DFO, indicating that the induction of LXRα occurred at the transcription level (Fig. 13E) (99,100). Six putative HREs are present in the LXRα gene promoter, to which HIF-1α was efficiently and preferentially recruited upon treatment with DFO (Fig. 13F). Together, these results demonstrated that HIF-1α is induced under hypoxia and transcriptionally activates LXRα by binding to the HREs in the LXRα gene promoter.

2.2. TO901317 induces protein stability and transcriptional activation of HIF-1α

Next, it was tested whether LXRα was involved in hypoxia signaling in primary human macrophages and murine RAW 264.7 cells. Treatment of both cell types with TO901317 increased the level of HIF-1α protein and its target VEGF, along with the induction of LXRα, in a dose-dependent manner (Fig. 14A). Overexpression of LXRα in RAW 264.7 cells increased the level of HIF-1α protein to the same extent as treatment with DFO (Fig. 14B). Knockdown of LXRα or LXRα/β using si-RNA completely abolished the induction of HIF-1α, indicating that the induction of HIF-1α was LXR-dependent (Fig. 14C). A reporter gene analysis using the HRE-tk-Luc further confirmed that LXRα was involved in the activation of HIF-1α (Fig. 14D). In the presence of TO901317, VEGF, LXRα and LXRβ mRNA levels were greatly increased; however, HIF-1α mRNA levels were unchanged, indicating that the induction of HIF-1α was achieved at the posttranscriptional level (Fig. 14E).

2.3. Activation of LXRα enhances HIF-1α stability

Next, it was tested whether LXRα enhanced the stability of the HIF-1α protein. For this purpose, it used cycloheximide, an inhibitor of de novo protein synthesis. Treatment with TO901317 or overexpression of LXRα in RAW 264.7 cells blocked degradation of HIF-1α, which was similar to the effect of hypoxia (Fig. 15A). The proteasomal inhibitor, MG132, strongly increased the amount of ubiquitinated HIF-1α. Overexpression of LXRα as well as treatment with TO901317 decreased the ubiquitinated HIF-1α to the same extent as hypoxia in RAW 264.7 cells (Fig. 15B). It was further investigated whether LXRα reduced the binding of HIF-1α to prolyl hydroxylases (PHDs), because HIF-1α undergoes proteasomal degradation after prolyl hydroxylation (91). The amount of HIF-1α bound to PHDs was largely decreased in the presence of LXRα or under hypoxia (Fig. 15C). Together, these results indicate that a positive activation loop between the hypoxia-mediated LXRα induction and the LXRα-induced activation of HIF-1α was generated under hypoxic conditions in macrophages.

2.4. LXRα interacts with HIF-1α in the nucleus

To further characterize the cross-talk between LXRα and HIF-1α, it was examined whether these proteins were physically associated. First, LXRα and HIF-1α were distributed in the nucleus under hypoxia or in the presence of TO901317 (Fig. 16A). A coimmunoprecipitation assay as well as a mammalian two-hybrid assay using the Gal4-driven luciferase reporter demonstrated that LXRα and HIF-1α physically interacted (Fig. 16B and 16C). It was delineated the domains of interaction using the truncated FLAG-tagged LXRα and the GST-fused HIF-1α (90). The coimmunoprecipitation experiments revealed that the oxygen-dependent degradation domain of HIF-1α bound to LXRα, whereas the ligand-binding domain (LBD) of LXRα served as the binding site for HIF-1α (Fig. 16D). The importance of this binding was indicated by the LBD of LXRα being sufficient to induce the increases in protein levels as well as transcriptional activity of HIF-1α (Fig. 16E and 16F).

2.5. LXRα increases the transactivation function of HIF-1α

Next, it was examined whether LXRα enhanced the transactivation function of HIF-1α, using a Gal4-driven luciferase reporter system. The full-length and LBD but not the N-terminus or DNA-binding domains of LXRα strongly enhanced Gal4-HIF-1α-induced reporter activity. However, the activity of Gal4-LXRα was not altered by HIF-1α (Fig. 17A). Consistent with this result, a ChIP assay showed that LXRα, HIF-1α and the coactivator, CREB binding protein (CBP), were able to bind to HREs in the promoter of HIF-1α target genes such as Glut-1 and erythropoietin (Fig. 17B). This result indicates that the physical interaction of HIF-1α and LXRα may enhance the transactivation function of HIF-1α by recruiting CBP onto the promoter of HIF-1α target genes.

2.6. The expression of LXRα and HIF-1α in atherosclerotic lesions

Next, it was examined whether lipogenesis increased in macrophages as a consequence of the positive cross-talk between LXRα and HIF-1α. Hypoxia and TO901317 treatment led to synergistic lipid accumulation in RAW 264.7 cells (Fig.

18A). Importantly, knockdown of LXRα or HIF-1α using si-RNA largely blocked the lipid accumulation induced by hypoxia or TO901317 treatment in RAW 264.7 cells (Fig. 18B). Hypoxia induced by DFO or TO901317 treatment significantly increased the amount of triglyceride in these cells. In addition, DFO and TO901317 treatment increased the levels of total and LDL cholesterol; however, the level of HDL cholesterol was reduced. Co-treatment with DFO and TO901317 further enhanced the levels of triglyceride and LDL cholesterol in RAW 264.7 cells (Fig. 18C).

2.7. Enhances in expression of lipogenic genes under hypoxia or after LXR ligand treatment

The expression of representative lipogenic genes, such as ADRP and SCD-1, was also increased by treatment of macrophages with DFO or TO901317. The induction of expression of these genes was efficiently inhibited by transfection of si-RNAs or by treatment with the LXR antagonist, 22(*S*)-HC (Fig. 20).

2.8. Enhances in expression of LXRα and HIF-1α by inflammatory responses

Proinflammatory cytokines such as Interleukin-1β (IL-1β) and tumor necrosis factor α (TNFα) induce the expression of HIF-1α in inflammatory lesions. Therefore, it was tested whether the positive cross-talk between LXRα and HIF-1α contributed to the cytokine-induced HIF-1α expression. As reported previously, IL-1β or TNFα increased the expression of HIF-1α protein as well as important proinflammatory signaling molecules such as inducible nitric oxide synthase and cyclooxygenase-2. Interestingly, the expression of LXRα, SREBP-1c and FAS increased in a similar manner (Fig. 21A). The mRNA levels of these genes and VEGF increased; however, the level of HIF-1α mRNA did not (Fig. 21B). Transfection of si-LXRα effectively decreased the levels of HIF-1α and LXRα protein, suggesting that LXRα plays an important role in the cytokine-induced inflammatory responses mediated by HIF-1α (Fig. 21C).

2.9. The expression of LXRα and HIF-1α in atherosclerotic lesions

Finally, the protein expression of HIF-1α and LXRα in atherosclerotic lesions was examined in the specimens obtained from patients with atherosclerosis. Immunohistochemical staining of LXRα and HIF-1α showed that each protein was localized in the monocytes in the atheroma (Fig. 22A). Double immunofluorescence staining revealed that expression of LXRα and HIF-1α largely overlapped in the region where the macrophage surface protein, CD68, was expressed (Fig. 22B).

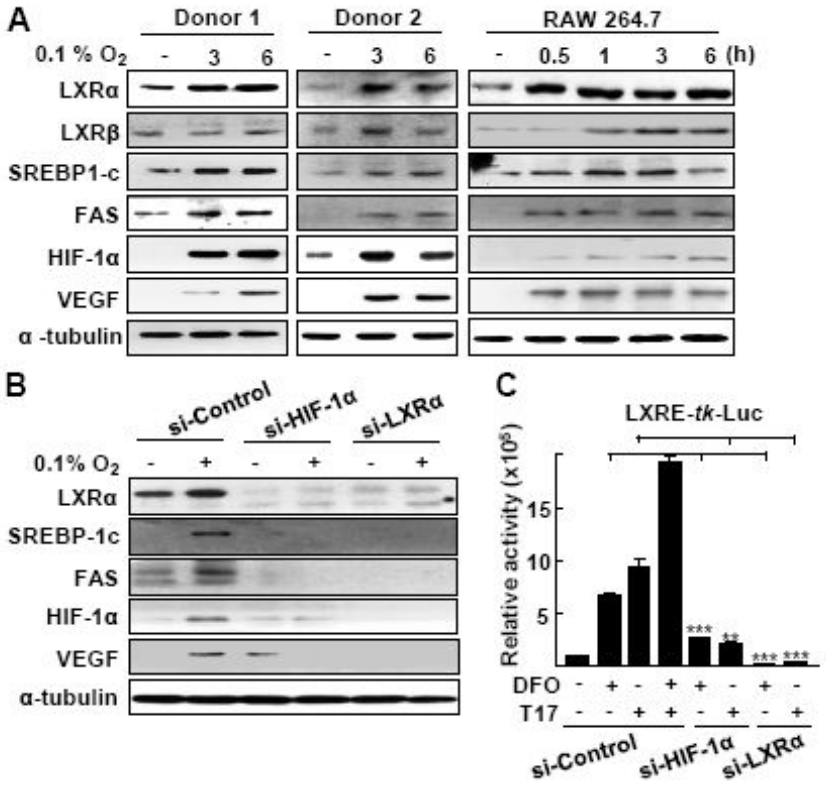
A
Donor 1
Donor 2
RAW 264.7
0.1 % O2
- 3 6
- 3 6
- 0.5 1 3 6 (h)
LXRα
LXRβ
SREBP1-c
FAS
HIF-1α
VEGF
α -tubulin
B
si-Control
si-HIF-1α
si-LXRα
0.1% O2
- + - + - +
LXRα
SREBP-1c
FAS
HIF-1α
VEGF
α-tubulin
C
LXRE-tk-Luc
Relative activity (x10³)
15
10
5
***
**
***
***
DFO - + - + + - + -
T17 - - + + - + - +
si-Control
si-HIF-1α
si-LXRα

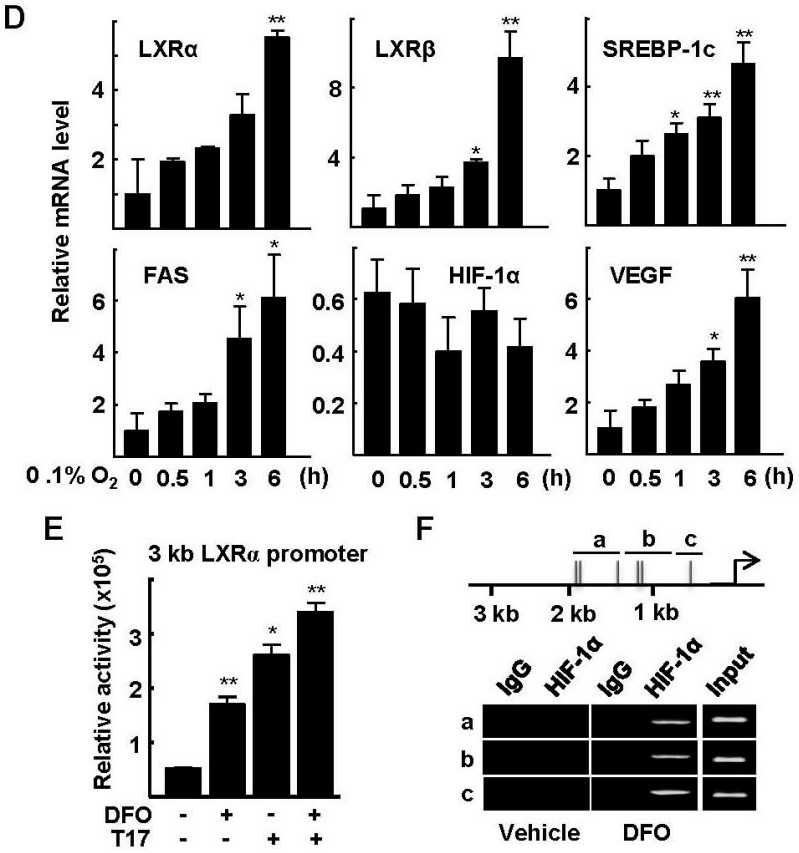
D
LXRα
LXRβ
SREBP-1c
FAS
HIF-1α
VEGF
Relative mRNA level
0 .1% O2 0 0.5 1 3 6 (h)
E
3 kb LXRα promoter
Relative activity (x10^5)
DFO - + - +
T17 - - + +
F
a b c
3 kb 2 kb 1 kb
IgG HIF-1α IgG HIF-1α Input
Vehicle DFO

Figure 13. LXRα was induced at the transcription-level in macrophages under hypoxia. (A) Human primary macrophages obtained from healthy donors and murine RAW 264.7 cells were incubated for indicated time under hypoxia. **(B)** RAW 264.7 cells were transfected with si-RNAs as indicated. Whole cell lysates were analyzed by western blotting. **(C)** RAW 264.7 cells were transfected with LXRE-Luc together with si-RNAs and treated with 1 μM TO901317 (T17) or 100 μM DFO for 24 h. **(D)** RAW 264.7 cells were incubated for the indicated time under hypoxia. Total RNA was prepared and analyzed for expression of the indicated transcripts by qRT-PCR using specific primers. **(E)** HeLa cells were transiently transfected with the human LXRα-promoter-Luc and were treated with 100 μM DFO and/or 1 μM T17 for 18 h. **(F)** Schematic representation of the human LXRα promoter investigated in this study. Sticks indicate the presence of putative HREs (upper). THP-1 cells were treated with 100 μM DFO for 12 h. DNA fragments that immunoprecipitated were amplified by PCR using primers that amplify the DNA fragment a, b and c as indicated (lower).

* $P < 0.05$, ** $P < 0.01$, and *** $P < 0.001$ (n=3)

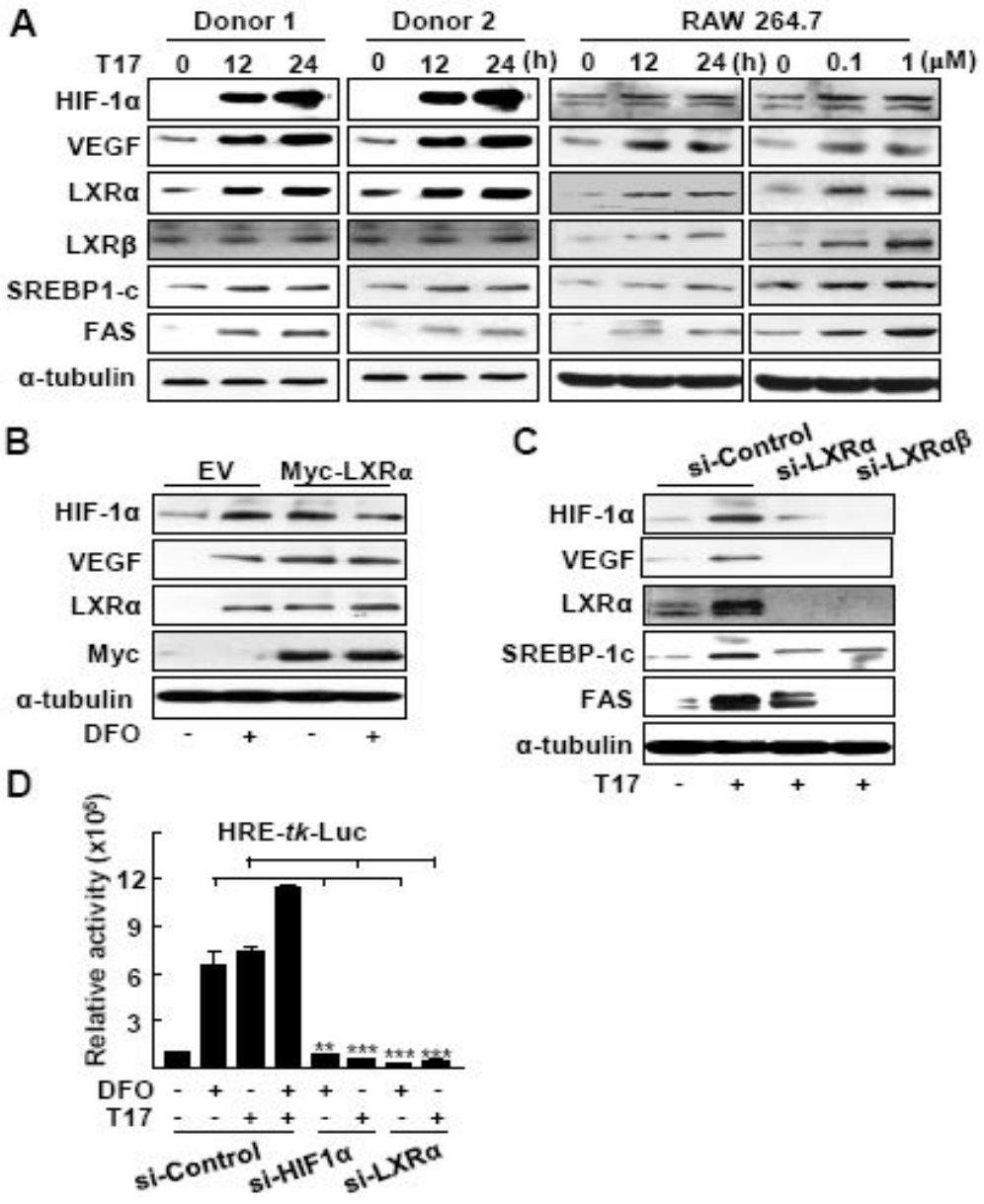
A
Donor 1
Donor 2
RAW 264.7
T17
0 12 24 0 12 24 (h) 0 12 24 (h) 0 0.1 1 (μM)
HIF-1α
VEGF
LXRα
LXRβ
SREBP1-c
FAS
α-tubulin
B
EV
Myc-LXRα
HIF-1α
VEGF
LXRα
Myc
α-tubulin
DFO - + - +
C
si-Control
si-LXRα
si-LXRαβ
HIF-1α
VEGF
LXRα
SREBP-1c
FAS
α-tubulin
T17 - + + +
D
HRE-tk-Luc
Relative activity (x10⁵)
12
9
6
3
**
***
***
***
DFO - + - + + - + -
T17 - - + + - + - +
si-Control
si-HIF1α
si-LXRα

Figure 14. Activation of LXRα enhances HIF-1α at protein-level not at mRNA-level. (A) Human primary macrophages and RAW 274.7 cells were treated 1 μM TO901317 (T17) for the indicated time or with the indicated concentration for 24 h. **(B)** RAW 264.7 cells were transfected with Myc-LXRα or empty vector (EV), and were incubated with 100 μM DFO for 12 h. **(C)** RAW 264.7 cells were transfected with si-RNAs as indicated and were treated with 1 μM T17 for 24 h. Whole cell lysates were analyzed by western blotting. **(D)** RAW 264.7 cells were transfected with HRE-tk-Luc together with si-RNAs. Transfected cells were incubated with 1 μM T17 for 24 h or 100 μM DFO for 12 h.

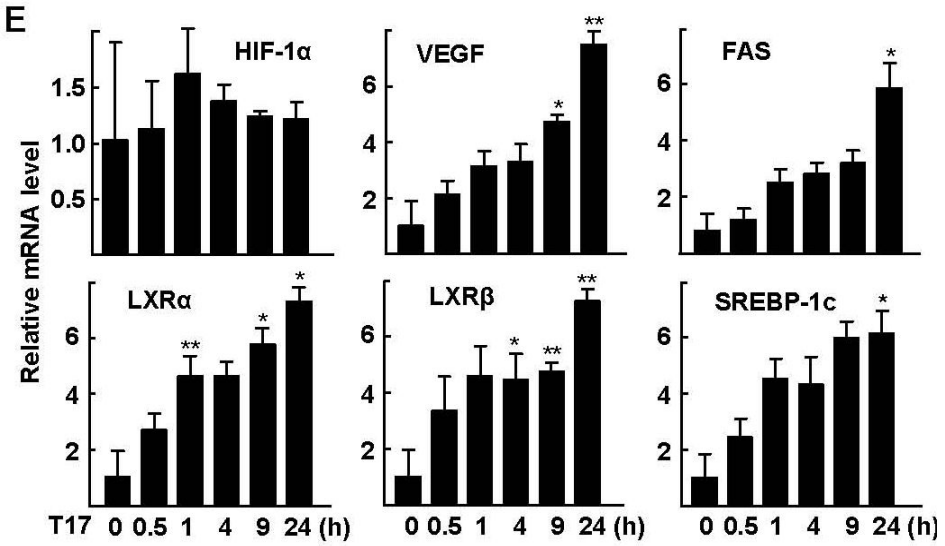
E
HIF-1α
VEGF
FAS
LXRα
LXRβ
SREBP-1c
Relative mRNA level
1.5
1.0
0.5
6
4
2
*
**
T17 0 0.5 1 4 9 24 (h)
0 0.5 1 4 9 24 (h)

Figure 14. Continued

(E) RAW 264.7 cells were treated with 1 μM T17 for the indicated period. Total RNA was prepared and analyzed for expression of the indicated transcripts by qRT-PCR. * $P < 0.05$, ** $P < 0.01$, and *** $P < 0.001$ (n=3)

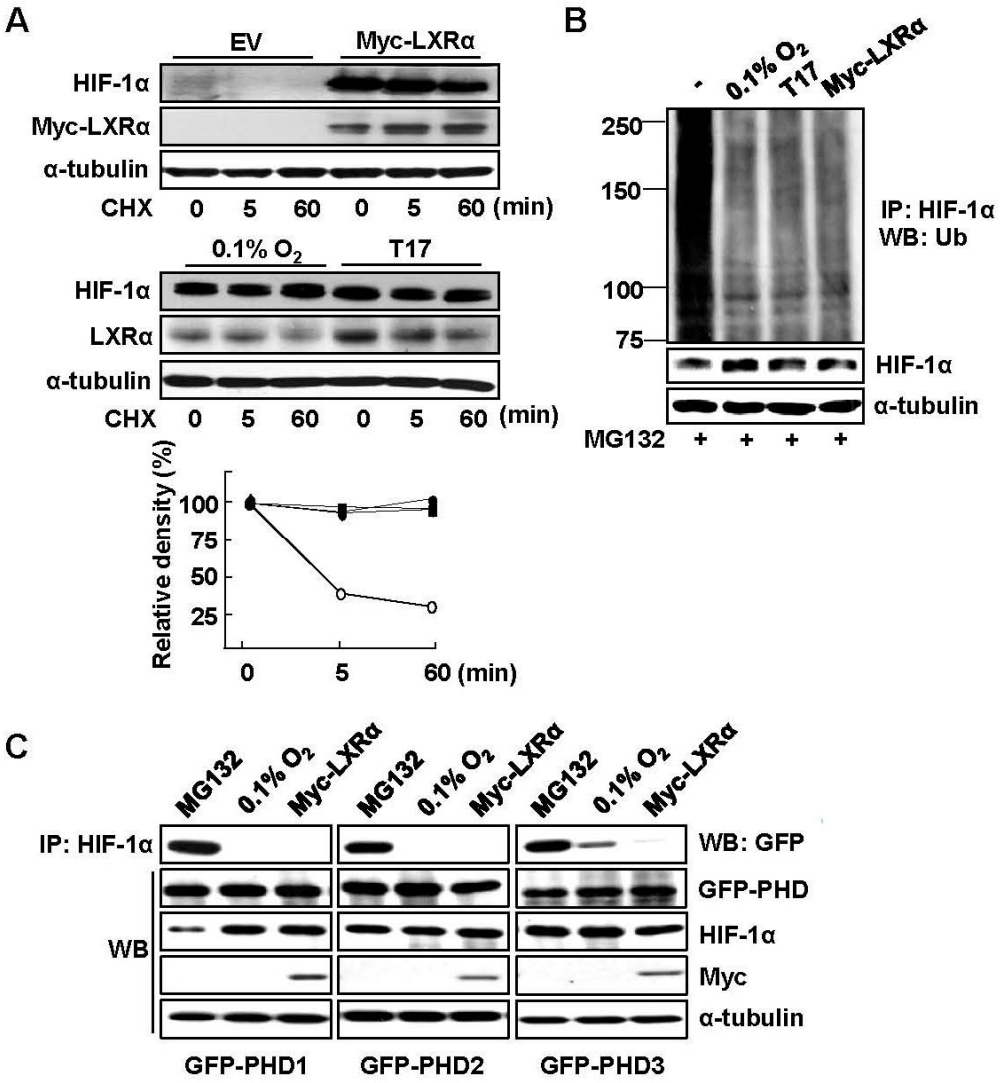
A
EV
Myc-LXRα
HIF-1α
Myc-LXRα
α-tubulin
CHX 0 5 60 0 5 60 (min)
0.1% O2
T17
HIF-1α
LXRα
α-tubulin
CHX 0 5 60 0 5 60 (min)
Relative density (%)
100
75
50
25
0 5 60 (min)
B
- 0.1% O2 T17 Myc-LXRα
250
150
100
75
IP: HIF-1α
WB: Ub
HIF-1α
α-tubulin
MG132 + + + +
C
MG132 0.1% O2 Myc-LXRα MG132 0.1% O2 Myc-LXRα MG132 0.1% O2 Myc-LXRα
IP: HIF-1α
WB: GFP
WB
GFP-PHD
HIF-1α
Myc
α-tubulin
GFP-PHD1 GFP-PHD2 GFP-PHD3

Figure 15. LXRα suppresses degradation of HIF-1α by blocking ubiquitination. **(A)** RAW 264.7 cells were transfected with empty vector (EV) or expression vector encoding Myc-LXRα. Cells transfected with EV were treated with 1 μM T17 or incubated under hypoxia for 12 h. At the end of treatment, 10 μM cycloheximide (CHX) was added for the indicated time period. Expression of the indicated proteins was analyzed by western blot analysis. The density of each protein band was determined with an image analysis system and normalized to that of the corresponding α-tubulin. **(B)** RAW 264.7 cells were transfected with EV or Myc-LXRα together with HA-ubiquitin (Ub). Cells transfected with EV were treated with 0.1% O2 for 12 h or 1 μM TO901317 (T17) for 24 h. And then cells were treated with 10 μM MG132 for 3 h before being harvested. Whole cell lysates were immunoprecipitated (IP) and analyzed by western blot analysis (WB). **(C)** NIH3T3 cells were transfected with expression vectors encoding GFP-PHD1, GFP-PHD2, and GFP-PHD3 with or without pCMV-Myc-LXRα as indicated. Transfected cells were incubated under hypoxia or normoxia for 12 h. Cells were treated with or without 10 μM MG132 for 3 h before being harvested. Whole cell lysates were IP and analyzed by WB.

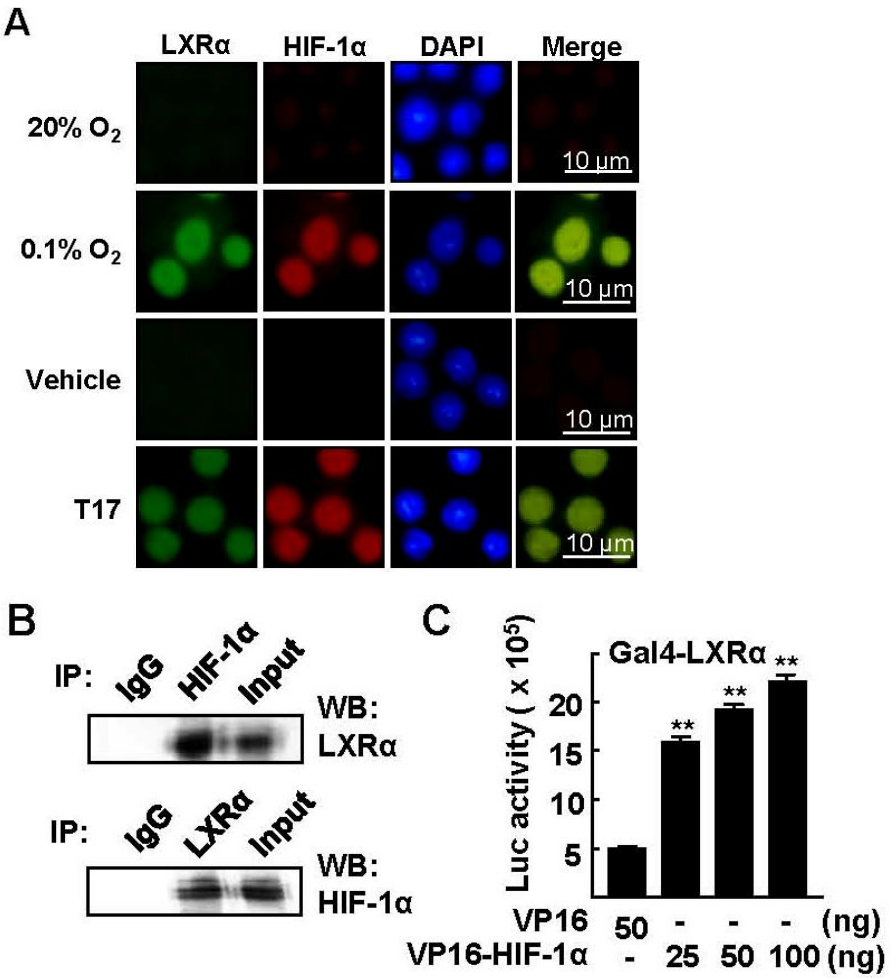
A
LXRα
HIF-1α
DAPI
Merge
20% O2
0.1% O2
Vehicle
T17
10 μm
B
IP:
IgG
HIF-1α
Input
WB:
LXRα
IP:
IgG
LXRα
Input
WB:
HIF-1α
C
Gal4-LXRα
Luc activity (x 10^5)
20
15
10
5
**
VP16 50 - - - (ng)
VP16-HIF-1α - 25 50 100 (ng)

Figure 16. LXRα interacts with HIF-1α in the nucleus. (A) RAW 264.7 cells were exposed with under hypoxia for 12 h or 1 μM TO901317 (T17) for 24 h. The end of treatment, cells were fixed, and expression of LXRα and HIF-1α was visualized by immunocytochemistry. **(B)** RAW 264.7 cells incubated under hypoxia for 12 h. Whole cell lysates were immunoprecipitated (IP) with the indicated antibodies, and precipitates were probed by western blot (WB) analysis. **(C)** RAW 264.7 cells were transfected Gal4-*tk*-Luc and pGal4-LXRα with increasing amount of VP16-HIF-1α. ** $P < 0.01$ (n=3)

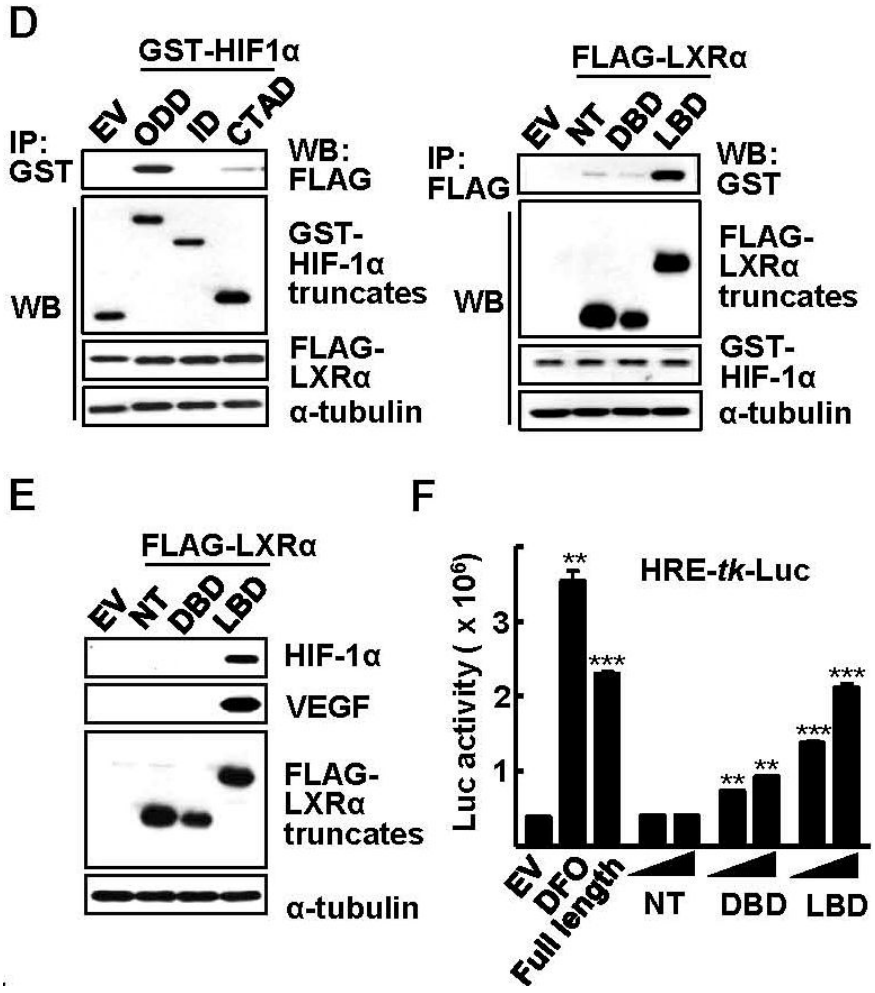
D
GST-HIF1α
EV
ODD
ID
CTAD
IP: GST
WB: FLAG
WB
GST-HIF-1α truncates
FLAG-LXRα
α-tubulin
FLAG-LXRα
EV
NT
DBD
LBD
IP: FLAG
WB: GST
WB
FLAG-LXRα truncates
GST-HIF-1α
α-tubulin
E
FLAG-LXRα
EV
NT
DBD
LBD
HIF-1α
VEGF
FLAG-LXRα truncates
α-tubulin
F
HRE-tk-Luc
Luc activity (x 10^6)
1
2
3
**
***
EV
DFO
Full length
NT
DBD
LBD

Figure 16. Continued. (D) RAW 264.7 cells were transfected with expression vectors encoding GST-HIF-1α (left) or FLAG-LXRα (right) with the indicated LXRα or HIF-1α truncates, respectively. Whole cell lysates were immunoprecipitated and analyzed by WB as indicated. **(E)** RAW 264.7 cells were transfected with FLAG-LXRα_{NT}, FLAG-LXRα_{DBD}, or FLAG-LXRα_{LBD}. **(F)** RAW 264.7 cells were transfected with HRE-*tk*-luc and the indicated expression vector for LXRα truncates, and were treated with 100 μM DFO for 24 h. ** $P < 0.01$, and *** $P < 0.001$ (n=3)

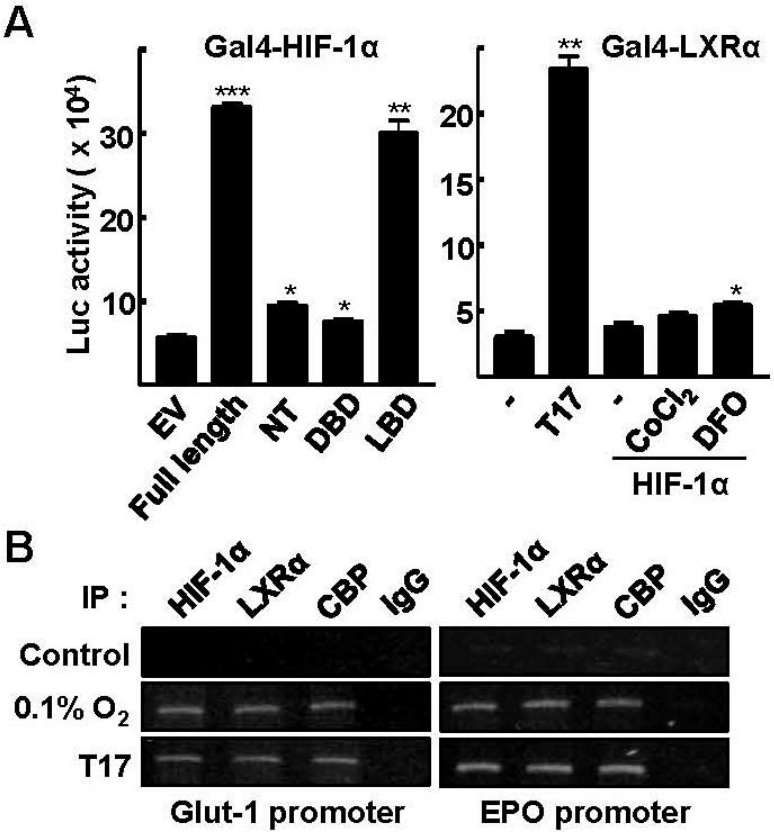
A
Gal4-HIF-1α
Gal4-LXRα
Luc activity (x 10⁴)
30
20
10
20
15
10
5
***
**
*
*
**
*
EV
Full length
NT
DBD
LBD
-
T17
-
CoCl₂
DFO
HIF-1α
B
IP :
HIF-1α
LXRα
CBP
IgG
HIF-1α
LXRα
CBP
IgG
Control
0.1% O₂
T17
Glut-1 promoter
EPO promoter

Figure 17. LXRα enhances transactivation function of HIF-1α. (A) NIH3T3 cells were transfected with Gal4-*tk*-luc and pGal4-HIF-1α together with the indicated LXRα truncates (left). Or cells were transfected with pGal4-LXRα and HIF-1α expression vector, and were treated with 1 μM TO901317 (T17), 100 μM $CoCl_2$, or 100 μM DFO (right). * $P < 0.05$, ** $P < 0.01$, and *** $P < 0.001$ (n=3) **(B)** RAW 264.7 cells were treated with 1 μM T17 or 0.1% O_2 for 12 h. DNA fragments that contain flanking region of the HIF-1α binding sites on the mouse promoter of Glut-1 and erythropoietin (EPO) genes were immunoprecipitated with the indicated antibodies were amplified by PCR.

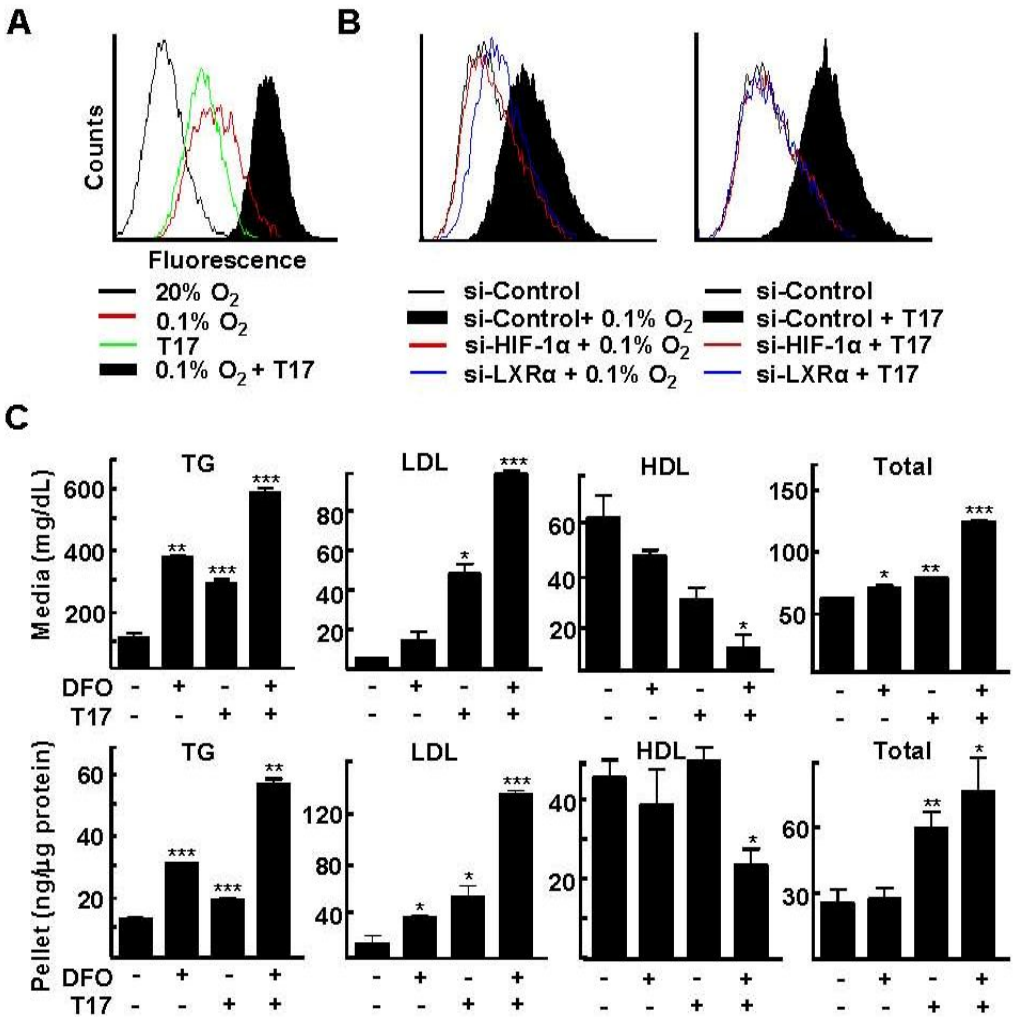
A
Counts
Fluorescence
20% O2
0.1% O2
T17
0.1% O2 + T17
B
si-Control
si-Control+ 0.1% O2
si-HIF-1α + 0.1% O2
si-LXRα + 0.1% O2
si-Control
si-Control + T17
si-HIF-1α + T17
si-LXRα + T17
C
Media (mg/dL)
TG
LDL
HDL
Total
DFO
T17
Pellet (ng/μg protein)
TG
LDL
HDL
Total
DFO
T17

Figure 18. Hypoxia and TO901317 induce triglyceride-rich lipogenesis in macrophages. (A) RAW 264.7 cells were incubated under hypoxia and/or treated with 1 μM TO901317 (T17). **(B)** RAW 264.7 cells were transfected with si-RNAs, and were treated with 0.1% O_2 for 24 h and/or 1 μM T17 for 96 h. At the end of treatment, lipid droplets were stained using Nile-red, and fluorescence was determined by flow cytometry. **(C)** Quantification of the pool of lipid droplets in RAW 264.7 cells. Cells were incubated with 100 μM DFO for 12 h and 1 μM TO901317 for 48 h. Cell pellets and culture media were analyzed for triglycerides, LDL (LDL and VLDL), HDL, and total cholesterol. * $P < 0.05$, ** $P < 0.01$, and *** $P < 0.001$ (n=3)

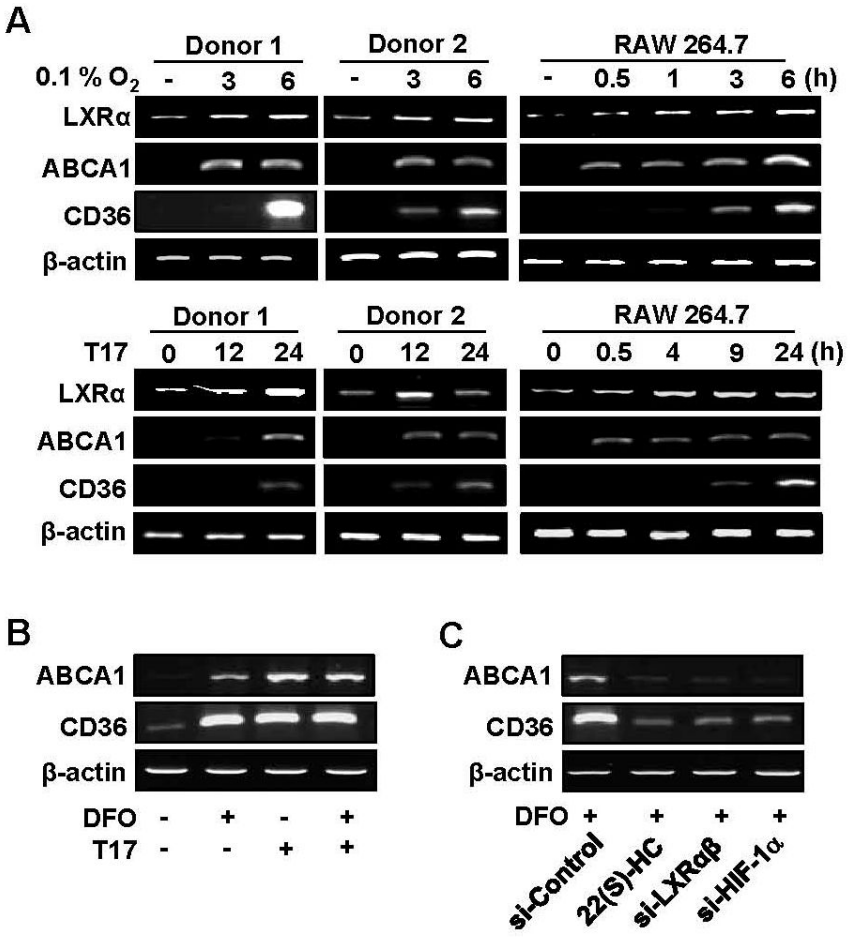
A
Donor 1
Donor 2
RAW 264.7
0.1 % O2
- 3 6
- 3 6
- 0.5 1 3 6 (h)
LXRα
ABCA1
CD36
β-actin
Donor 1
Donor 2
RAW 264.7
T17
0 12 24
0 12 24
0 0.5 4 9 24 (h)
LXRα
ABCA1
CD36
β-actin
B
ABCA1
CD36
β-actin
DFO - + - +
T17 - - + +
C
ABCA1
CD36
β-actin
DFO + + + +
si-Control
22(S)-HC
si-LXRαβ
si-HIF-1α

Figure 19. Increases in expression level of ABCA1, ABCG1, and CD36 under hypoxia or after TO901317 treatment. (A) Human primary macrophages and RAW 264.7 cells were incubated for the indicated time in 0.1% O_2 or 1 μM TO901317 (T17). **(B)** RAW 264.7 cells were incubated with 100 μM DFO for 12 h or 1 μM T17 for 24 h. **(C)** RAW 264.7 cells were transfected with the indicated si-RNAs. After 3 h of transfection, the cells were treated with 22(*S*)-hydroxycholesterol (HC) or vehicle for 24 h. Total RNA was prepared and analyzed for expression of the indicated transcripts by RT-PCR. One representative of at least three independent experiments with similar results is shown.

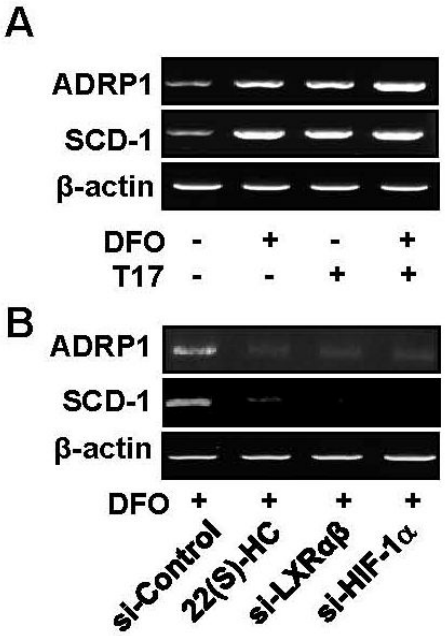
A
ADRP1
SCD-1
β-actin
DFO - + - +
T17 - - + +
B
ADRP1
SCD-1
β-actin
DFO + + + +
si-Control
22(S)-HC
si-LXRαβ
si-HIF-1α

Figure 20. Increases in expression level of ADRP1 and SCD-1 under hypoxia or after TO901317 treatment. (A) RAW 264.7 cells were incubated with 100 μM DFO for 12 h or 1 μM TO901317 (T17) for 24 h. **(B)** RAW 264.7 cells were transfected with the indicated si-RNAs. After 3 h of transfection, the cells were treated with 22(S)-hydroxycholesterol (HC) or vehicle for 24 h. Total RNA was prepared and analyzed for expression of the indicated transcripts by RT-PCR.

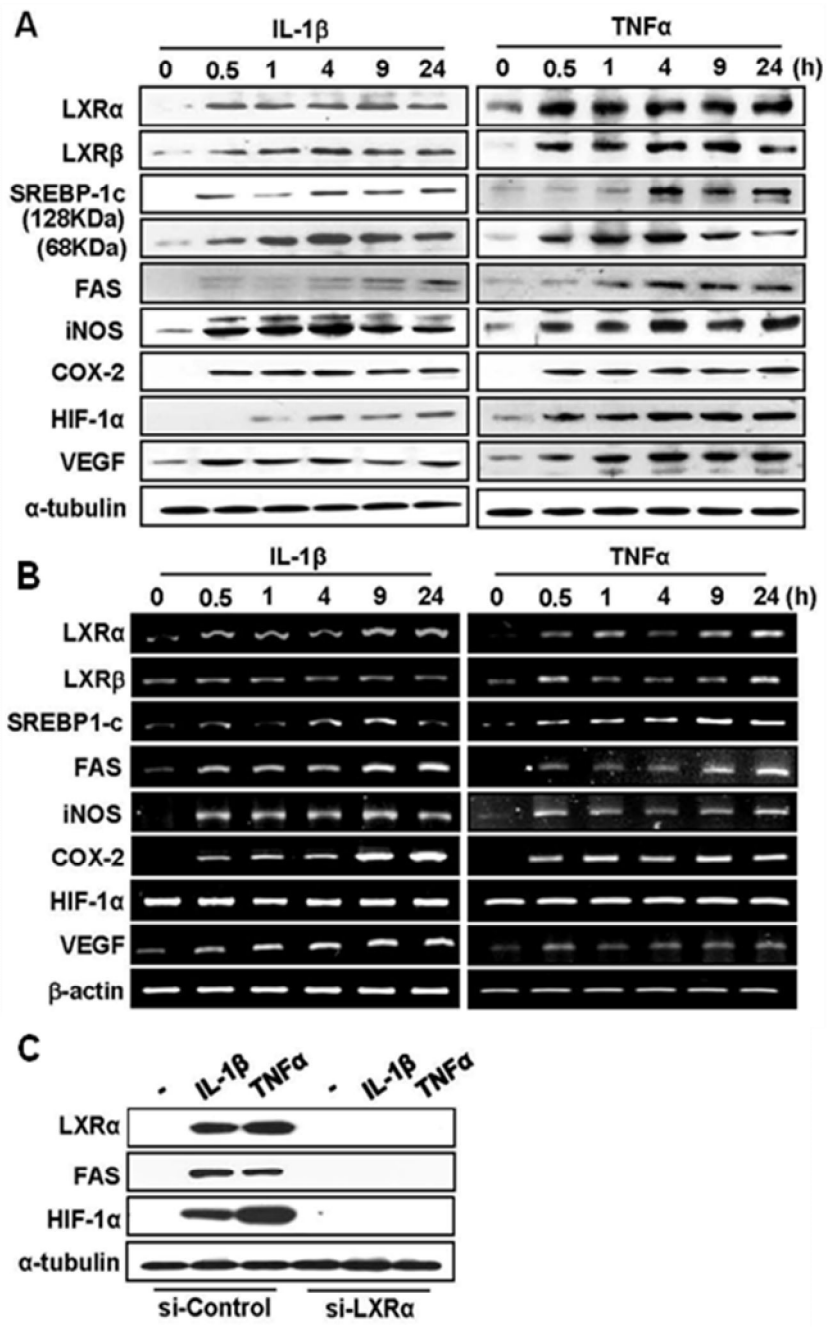
A
IL-1β
TNFα
0 0.5 1 4 9 24 (h)
LXRα
LXRβ
SREBP-1c
(128KDa)
(68KDa)
FAS
iNOS
COX-2
HIF-1α
VEGF
α-tubulin
B
IL-1β
TNFα
0 0.5 1 4 9 24 (h)
LXRα
LXRβ
SREBP1-c
FAS
iNOS
COX-2
HIF-1α
VEGF
β-actin
C
- IL-1β TNFα - IL-1β TNFα
LXRα
FAS
HIF-1α
α-tubulin
si-Control
si-LXRα

Figure 21. Increases in expression level of LXRα and HIF-1α after treatment of inflammatory cytokines. (A) RAW 264.7 cells were treated with 10 ng/ml IL-1β or TNFα for the indicated period. **(B)** Total RNA was prepared and analyzed for expression of the indicated transcripts by RT-PCR using specific primers. **(C)** RAW 264.7 cells were transfected with si-control or si-LXRα and treated with 10 ng/ml IL-1β or TNFα for 24 h. The whole cell lysates were analyzed for expression of the indicated proteins by western blot analysis.

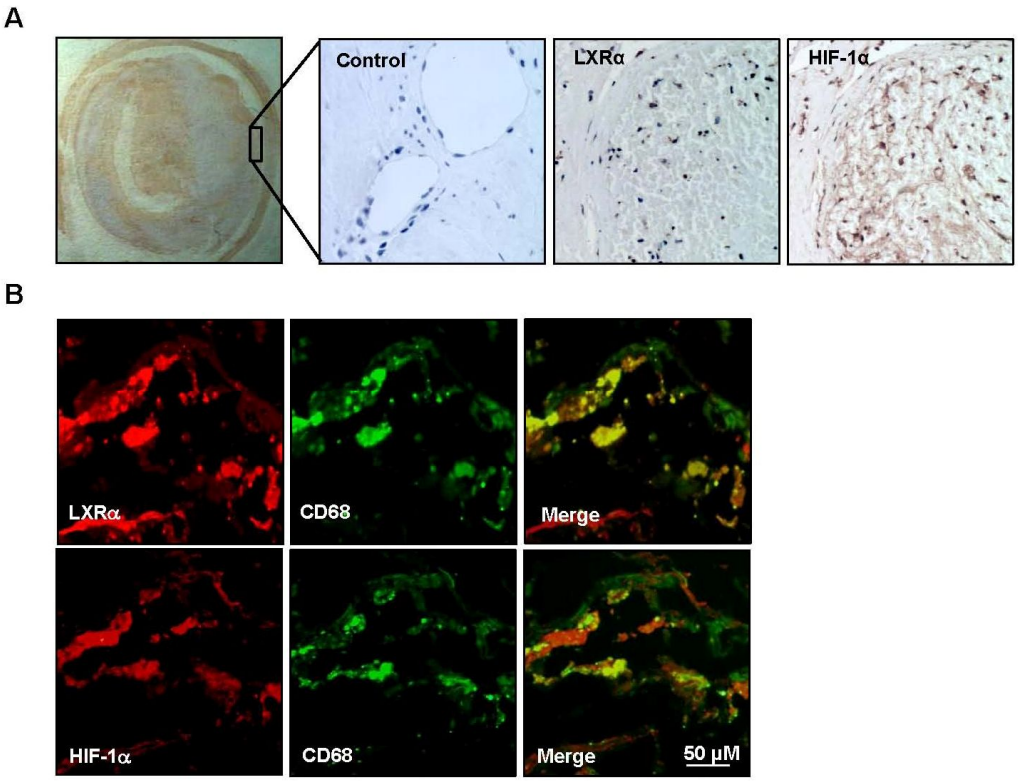
A
Control
LXRα
HIF-1α
B
LXRα
CD68
Merge
HIF-1α
CD68
Merge
50 μM

Figure 22. Both LXRα and HIF-1α are distributed in foam cells of human atherosclerotic lesions. (A) Human vascular sections showed specific staining for LXRα and HIF-1α by immunohistochemistry. Original magnification, X400 **(B)** Immunofluorescence staining of LXRα and HIF-1α in human atherosclerotic lesions. Human vascular sections showed specific staining with anti-CD68 mAb for macrophages. Original magnification X100.

V. DISCUSSION

There is abundant evidence to suggest that the increased liver triglyceride levels lead to increased liver damage by effects such as oxidative stress in the hepatocytes of animals and human beings. The increased hepatic lipogenesis is able to induce liver inflammation through inducing the production of proinflammatory cytokines. It is known that HBV-induced inflammatory response associates with the progression of liver damage. Interestingly, my results showed that lipid accumulation in HBx-TG mice (Fig. 4). Therefore, in this study, because of the importance of HBV-induced lipid accumulation, the mechanisms of hepatic steatosis by HBV infection studied intensively.

Such as regulation of lipogenesis by LXR in liver, LXRs play a pivotal role in the lipid homeostasis of macrophage. The role of macrophage in atherogenesis has been a topic of great interest associated with foam cell formation. Hypoxic regions in atherosclerotic lesions contain large numbers of foam cells, revealing that these cells experience hypoxia during the development of atherosclerosis. In this study, I discussed the positive feedback circuit consisting of cross-talk between HIF-1α and LXRα induced by hypoxia in macrophages, leading to foam-cell formation.

1. Roles of LXRs in HBx-induced lipogenesis in HBV-associated HCC

1.1. Development of lipogenesis in tumor

Increasing evidence indicates that hepatic lipogenesis is related to hepatic fibrosis, inflammation, apoptosis, and human cancer. In particular, many tumor tissues including colon, breast, and lung, undergo events leading to fatty acid synthesis; therefore, these tumor tissues contain high levels of lipids, when compared with normal tissues (101-103). Upregulation of lipogenic enzymes such as FAS, the key metabolic multienzyme responsible for the terminal catalytic step in fatty acid synthesis, represents a phenotypic alteration in many human malignancies (102,103). Interestingly, gene expression profiles obtained by cDNA microarray analysis of HBV-infected mouse liver revealed that expression of genes that are involved in the biosynthesis and metabolism of fatty acids and steroids together with genes associated with cell cycle progression, were upregulated after HBV infection (98).

1.2. Development of LXR-dependent steatosis in HBV-induced HCC

Lipogenic enzymes such as FAS and acetyl-CoA carboxylase 1 are markedly induced in HCC (104). Here, it demonstrated that the transcriptional function of LXR was strongly enhanced by HBx in cell culture and in an HBx-transgenic mouse model, and that the expression of LXRβ, SREBP-1c, and FAS was significantly upregulated in liver specimens of HBV-associated HCC. These results suggest that the HBx-induced lipogenic pathways, including the activation of the LXR-SREBP-1c-FAS axis of lipogenic program, may play an important role in progression of hepatocarcinogenesis, and may provide diagnostic advantages as well as therapeutic targets for the HBV-associated HCC. Kim *et al*. (2007) reported that HBx induces lipogenesis through activation of SREBP-1 and PPARs (98). In the this study, it also observed that expression of SREBP-1c and all subtypes of PPARs was enhanced in the presence of HBx (Fig. 4 and 7). Importantly, it was demonstrated that knock-down of LXRα and/or LXRβ dramatically inhibited the expression and transcriptional activity of SREBP-1 and PPARs. Consistently, the HBx-induced

lipogenesis was largely decreased when expression of LXRα and LXRβ was repressed by RNA interference (Fig. 8). These results suggest that regulation of SREBP-1c and PPARs by HBx may be indirect and mediated by LXR, which indicates that LXR may be the main regulator of HBx-induced hepatic lipogenesis (Fig. 23). The fact that the retinoid X receptor, a heterodimer partner of LXR, directly interacts with HBx (105), may further provide a tool to effectively enhance the transcriptional activity of LXR - Retinoid X receptor heterodimers on promoters of the LXR target genes.

1.3. The potential role of the LXR pathway in HBV-associated metabolic syndromes

Chronic infection with HBV has been implicated in metabolic syndromes; HBx was shown to transactivate phosphoenolpyruvate carboxykinase, which is associated with gluconeogenesis and insulin resistance, and an increased prevalence of carotid atherosclerosis was found in HBV carriers in a large cohort study (104,106). Also,

LXR was implicated in insulin resistance and gluconeogenesis. Therefore, the potential role of the LXR pathway in HBV-associated metabolic syndromes warrants further investigation. Importantly, the transcriptional activity of LXR can be antagonized by small molecules, such as the polyunsaturated fatty acids docosahexaenoic acid and eicosapentaenoic acid (53). Interestingly, a rapid decline in endogenous fatty acid synthesis following FAS inhibition using chemical inhibitors significantly decreases cell proliferation in several types of tumor cells (102,103). Therefore, such compounds may be useful for targeting LXRα and/or FAS to repress HBV-associated hepatic steatosis, as well as the related symptoms resulting from HBV infection.

1.4. The role of HCV in hepatic steatosis

Similar to HBx, HCV core protein plays an important role in hepatic steatosis during pathogenesis of HCV infection. It enhances the de novo biosynthesis of fatty acids and triacylglycerol in vitro and induces hepatic steatosis in the core protein-

carrying transgenic mice (56,57,107). Potential mechanisms for the HCV core protein-induced hepatic steatosis have been elucidated at the molecular level. HCV core protein indirectly enhances SREBP-1c promoter activity by increasing the binding of LXRα/RXRα to the LXRE, which is markedly activated by treatment with the ligands for LXRα and RXRα (59). Particularly, the genotype-3a core upregulates the FAS promoter, which could contribute to a higher prevalence and severity of steatosis (108). These observations together with our results suggest that HBV and HCV utilize similar molecular tools for the modulation of lipogenesis. This implies that the LXR-mediated lipogenic pathway may be critical for pathogenesis of the hepatotropic and oncogenic viruses.

2. Roles of LXRs in hypoxia-induced foam cell formation in atherosclerotic lesion

2.1. Cross-talk between HIF-1α and LXRα in macrophage

Hypoxic regions in atherosclerotic lesions contain large numbers of foam cells, revealing that these cells experience hypoxia during the development of atherosclerosis. Here, I demonstrated that hypoxia induces a positive feedback circuit consisting of cross-talk between HIF-1α and LXRα, which results in enhanced lipogenesis in macrophages, leading to foam-cell formation. This finding was supported by immunohistochemical observations that HIF-1α and LXRα are codistributed in the macrophages within atherosclerotic lesions of patients with atherosclerosis. Therefore, I characterized the molecular details of the cross-talk between HIF-1α and LXRα. First, the transcription of LXRα was increased in the macrophages under hypoxia, which is achieved via the several HREs scattered in the promoter region of the LXRα gene. The reporter containing the 5′ upstream promoter

of LXRα was well activated under hypoxia and the binding of HIF-1α to the promoter region was demonstrated by a ChIP assay (Fig. 17E and 17F). This finding may explain why knockdown of HIF-1α inhibits the expression of LXRα, which was observed previously (49). Second, LXRα enhances the stability of the HIF-1α protein. This is achieved by the direct interaction of LXRα with HIF-1α, which diminishes the association of HIF-1α with PHDs (Fig. 15). Further binding of LXRα with HIF-1α recruits more CBP, which activates the transactivation function of HIF-1α (Fig. 17). Therefore, the environmental and intracellular stimuli that trigger HIF-1α or LXRα turn on this positive feedback circuit, which augments the hypoxia and lipogenic signaling pathways.

2.2. The role of LXR in foam-cell formation

The lipogenic function of LXRα in the liver is well established; however, the role of LXR in foam-cell formation is not yet clearly understood (8). Macrophages isolated from human atherosclerotic plaques predominantly contain cholesterol esters

with substantial amounts of triglyceride (109). Because a large amount of oxidized derivatives of cholesterol, oxysterols, known endogenous activators of LXR, are present in macrophage-derived foam cells or human atherosclerotic plaques (110–112), the transcriptional activity of LXRα can be activated to trigger downstream targets. Indeed, the activation of LXRα increases the expression of SREBP-1c and FAS, which leads to increased levels of triglyceride in RAW 264.7 cells (Fig. 14 and 18). The accumulation of cholesterol in the macrophages is associated with increased uptake and decreased efflux of cholesterol. In this study, it was found that the level of LDL increased, whereas the level of HDL decreased, in culture media when RAW 264.7 cells were incubated in the presence of TO901317 or under hypoxia (Fig. 18). This observation may be contradictory to the known function of LXRα because the reverse cholesterol transporters such as ABCA1 and ABCG1 are direct downstream targets of LXRα. However, it was also found that the expression of the scavenger receptor CD36 was increased under the same conditions, which may override the efflux of cholesterol by ABC transporters (Fig. 19) (113,114). Taken together, the

accumulation of potential LXR ligands and the resulting enhancement of hypoxic signaling in the atherosclerotic lesion may contribute to increases in the levels of cholesterol and triglyceride in the macrophages (Fig. 24).

2.3. The role of HIF-1α and LXRα in inflammatory response

Hypoxia induces the expression of a variety of proinflammatory cytokines, such as 15-lipoxygenase-2, eicosanoids, IL-1β, and TNFα (15,116). The cytokines may induce inflammatory responses involving the increased production of lipid droplets (117). Conversely, activation of LXRα by its oxysterol ligands stimulates mRNA synthesis and protein expression of TNFα (118). Interestingly, TNFα and VEGF are direct targets of LXRα, indicating that LXRα and HIF-1α signaling may be coupled with inflammatory responses in atherosclerotic lesions (118,119). Therefore, it assessed whether the positive feedback circuit of HIF-1α and LXRα activation described in foam-cell formation operated for inflammatory responses. Here showed that the increased expression of HIF-1α resulting from treatment with IL-1β and

TNFα induced the expression of lipogenic genes including LXRs and their target genes (Fig. 18A). Surprisingly, knockdown of LXRα effectively inhibited the HIF-1α protein levels (Fig. 18B). These observations support the notion that the hypoxia-induced inflammatory process is accompanied by the accumulation of lipids and that the positive feedback circuit of HIF-1α and LXRα in macrophage cells may be a key step in coordinating the cellular events that result in atherosclerotic lesions by linking inflammation and lipogenesis.

2.4. LXR is controversial in application of LXRα ligands for therapeutics

Trials of LXRα ligands as therapeutics for atherosclerosis have been controversial. Because genes involved in the efflux of cholesterol are direct downstream targets of LXRα, as described above, the level of cholesterol in the macrophages is expected to decrease with LXRα activation. In experimental animals, the constitutive activation of LXRα in the intestinal epithelium reduced atherosclerosis by decreasing intestinal cholesterol absorption, improving lipoprotein

composition, and stimulating reverse-cholesterol transport, which provided the rationale for LXR being an appealing drug target for atherosclerosis (81). However, administration of synthetic LXR ligands triggers the induction of the lipogenic pathway and elevates plasma triglyceride levels via SREBP-1. In Ldlr–/– mice, TO901317 increases mRNA for enzymes involved in fatty acid biosynthesis and produces massive hypertriglyceridemia (12,84,85). To complicate matters further, a pro-inflammatory role of LXRs was seen in primary human macrophages, which was in contrast to previous observations of LXRs as negative regulators of inflammatory gene expression (16,17). LXR activation augmented the production of inflammatory cytokines IL-12, TNF-α, IL-6, and IL-8 in human monocyte-derived immune cells (18). Here, my results reveal a new aspect of LXR action, which augments hypoxia-induced cellular signaling in the macrophages. The lipogenic and inflammatory responses associated with LXR activation may induce a vicious cycle of lipid production and inflammation in the macrophages, which contributes to the development of atherosclerotic lesions. Thus, the positive feedback circuit connecting

activation of HIF-1α and LXRα may represent a new potential target for the prevention of foam-cell formation and inflammation in arterial walls and further progression to atherosclerosis (Fig. 25).

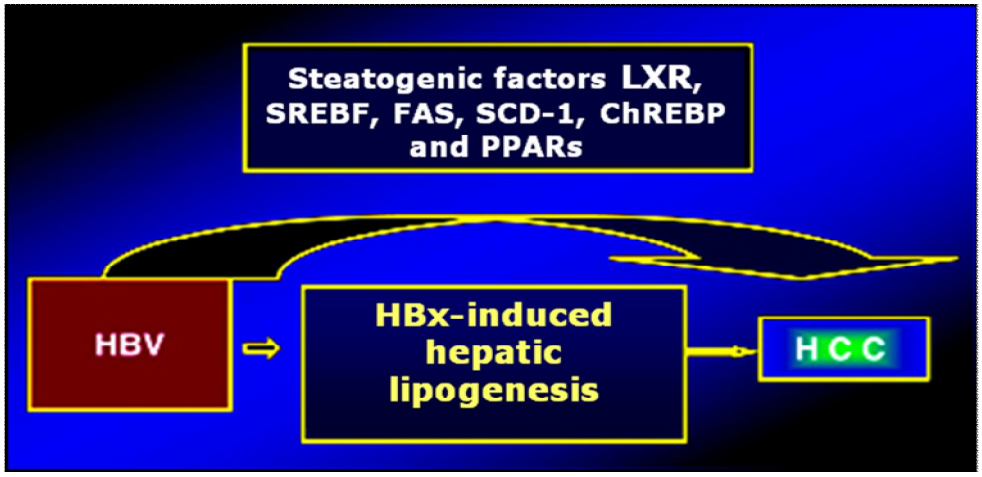

Figure 23. LXR-induced hepatic lipogenesis in development of HBV-associated human hepatocellular carcinoma.

Regulation of SREBP-1c and PPARs by HBx may be indirect and mediated by LXR, which indicates that LXR may be the main regulator of HBx-induced hepatic lipogenesis.

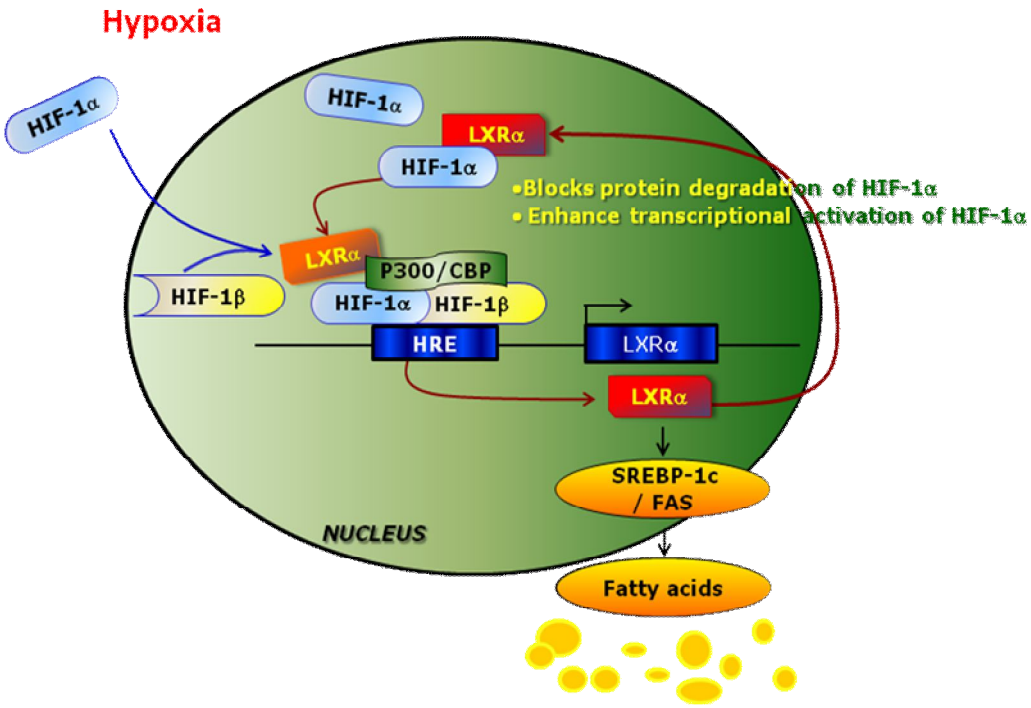

Figure 24. The positive feedback circuit of HIF-1α and LXRα.

The accumulation of potential LXR ligands and the resulting enhancement of hypoxic signaling in the atherosclerotic lesion may contribute to increases in the levels of cholesterol and triglyceride in the macrophages.

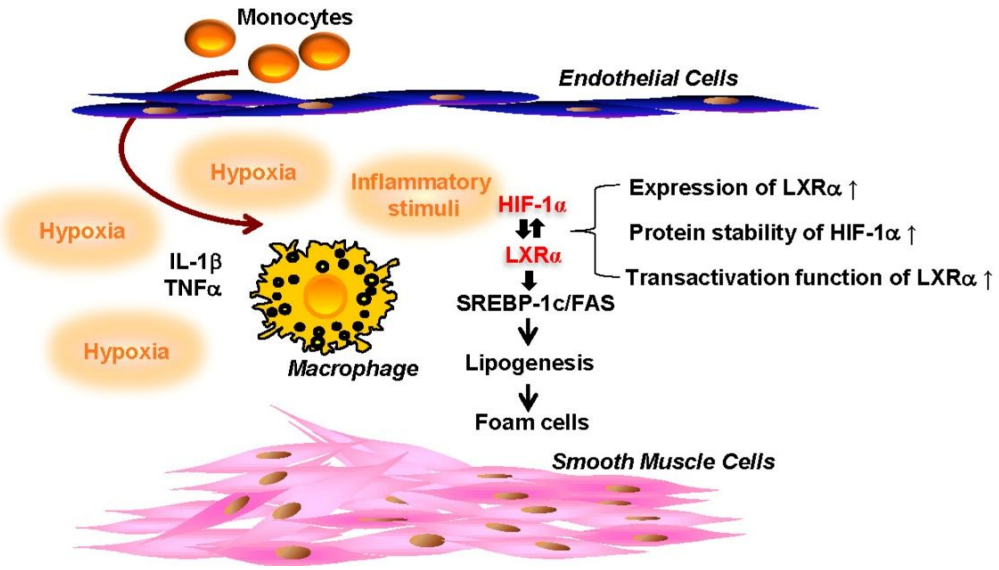

Figure 25. Schematic model for cross-talk of HIF-1α and LXRα in the foam cell formation of human atherosclerotic lesions.

The positive feedback circuit connecting activation of HIF-1α and LXRα may represent a new potential target for the prevention of foam-cell formation and inflammation in arterial walls and further progression to atherosclerosis.

VI. CONCLUSIONS

In this study, I showed that the role of liver X receptor in the pathogenesis of lipid metabolism disorder.

In study of liver, my results suggest that a novel association between LXR and HBx, which may provide important mechanisms of the HBV-induced hepatic lipogenesis and of the HBV-associated hepatic carcinogenesis. The conclusions obtained from the present study will extend our understanding of HBV-associated hepatocarcinogenesis and facilitate the development of new therapeutic strategies directed against HCC.

In study of macrophage, my results suggest that the positive-feedback regulation of transcriptional induction and protein stability of LXRα and HIF-1α have an important impact in the foam cell formation and development of atherosclerotic lesion. My studies provide a new insight for the function of LXRα in hypoxia signaling and suggest a potential strategy for the therapy of hypoxia-associated vascular diseases. Therefore, my results reveal a new aspect of LXR action, which lipogenic and inflammatory responses associated with LXR activation may turn on a

vicious cycle of lipid production and inflammation in the lipogenic metabolism abundant tissues, which contributes to the development of lipid metabolism associated disorder.

VII. REFERENCES

1. Baranowski M. Biological role of liver X receptors. J Physiol Pharmacol. 2008;59:31-55.

2. Chawla A, Repa JJ, Evans RM, Mangelsdorf DJ. Nuclear receptors and lipid physiology: opening the X-files. Science. 2001;30:1866-1870.

3. Alberti S, Steffensen KR, Gustafsson JA. Structural characterisation of the mouse nuclear oxysterol receptor genes LXRα and LXRβ. Gene. 2000;243:93-103

4. Wójcicka G, Jamroz-Wiśniewska A, Horoszewicz K, Bełtowski J. Liver X receptors (LXRs). Part I: structure, function, regulation of activity, and role in lipid metabolism. Postepy Hig Med Dosw. 2007 ;61:736-759.

5. Liu Y, Qiu de K, Ma X. Liver X receptors bridge hepatic lipid metabolism and inflammation. J Dig Dis. 2012;13:69-74.

6. Chawla A, Repa JJ, Evans RM, Mangelsdorf DJ. Nuclear receptors and lipid physiology: opening the X-files. Science. 2001;30:1866-1870.

7. Edwards PA, Kennedy MA, Mak PA. LXRs; oxysterol-activated nuclear receptors that regulate genes controlling lipid homeostasis. Vascul Pharmacol. 2002;38:249-256.

8. Schultz JR, Tu H, Luk A, Repa JJ, Medina JC, Li L. Role of LXRs in control of lipogenesis. Genes Dev. 2000;14: 2831-2838.

9. Kidani Y, Bensinger SJ. Liver X receptor and peroxisome proliferator-activated receptor as integrators of lipid homeostasis and immunity. Immunol Rev. 2012;249:72-83.

10. A-Gonzalez N, Bensinger SJ, Hong C, Beceiro S, Bradley MN, Zelcer N, Deniz J, Ramirez C, Díaz M, Gallardo G, de Galarreta CR, Salazar J, Lopez F, Edwards P, Parks J, Andujar M, Tontonoz P, Castrillo A. Apoptotic cells promote their own clearance and immune tolerance through activation of the nuclear receptor LXR. Immunity. 2009;31:245-258.

11. Bruhn KW, Marathe C, Maretti-Mira AC, Nguyen H, Haskell J, Tran TA, Vanchinathan V, Gaur U, Wilson ME, Tontonoz P, Craft N. LXR deficiency confers increased protection against visceral Leishmania infection in mice. PLoS Negl Trop Dis. 2010;4:e886.

12. Okazaki H, Goldstein JL, Brown MS, Liang G. LXR-SREBP-1c-phospholipid

transfer protein axis controls very low density lipoprotein (VLDL) particle size. J Biol Chem. 2010;285:6801-6810.

13. Grefhorst A, Elzinga BM, Voshol PJ, Plösch T, Kok T, Bloks VW, van der Sluijs FH, Havekes LM, Romijn JA, Verkade HJ, Kuipers F. Stimulation of lipogenesis by pharmacological activation of the liver X receptor leads to production of large, triglyceride-rich very low density lipoprotein particles. J Biol Chem. 2002;13:34182-34190.

14. Chisholm JW, Hong J, Mills SA, Lawn RM. The LXR ligand T0901317 induces severe lipogenesis in the db/db diabetic mouse. J Lipid Res. 2003;44:2039-2048.

15. Okazaki H, Goldstein JL, Brown MS, Liang G. LXR-SREBP-1c-phospholipid transfer protein axis controls very low density lipoprotein (VLDL) particle size. J Biol Chem. 2010;26:6801-6810.

16. Fontaine C, Rigamonti E, Pourcet B, Duez H, Duhem C, Fruchart JC, Chinetti-Gbaguidi G, Staels B. The nuclear receptor Rev-erbalpha is a liver X receptor (LXR) target gene driving a negative feedback loop on select LXR-induced pathways in

human macrophages. Mol Endocrinol. 2008;22:1797-1811.

17. Dai X, Ou X, Hao X, Cao D, Tang Y, Hu Y, Li X, Tang C. Effect of T0901317 on hepatic proinflammatory gene expression in apoE-/- mice fed a high-fat/high-cholesterol diet. Inflammation. 2007;30:105-117.

18. Töröcsik D, Baráth M, Benko S, Széles L, Dezso B, Póliska S, Hegyi Z, Homolya L, Szatmári I, Lányi A, Nagy L. Activation of liver X receptor sensitizes human dendritic cells to inflammatory stimuli. J Immunol. 2010;15:5456-5465.

19. C.P. Chuu. Modulation of liver X receptor signaling as a prevention and therapy for colon cancer. Med. Hypothese. 2011;76:697−699

20. Villablanca EJ, Raccosta L, Zhou D, Fontana R, Maggioni D, Negro A, Sanvito F, Ponzoni M, Valentinis B, Bregni M, Prinetti A, Steffensen KR, Sonnino S, Gustafsson JA, Doglioni C, Bordignon C, Traversari C, Russo V. Tumor-mediated liver X receptor-alpha activation inhibits CC chemokine receptor-7 expression on dendritic cells and dampens antitumor responses. Nat Med. 2010;16:98-105.

21. Fukuchi J, Kokontis JM, Hiipakka RA, Chuu CP, Liao S. Antiproliferative effect

of liver X receptor agonists on LNCaP human prostate cancer cells. Cancer Res. 2004;64:7686-7689.

22. Chuu CP, Hiipakka RA, Kokontis JM, Fukuchi J, Chen RY, Liao S. Inhibition of tumor growth and progression of LNCaP prostate cancer cells in athymic mice by androgen and liver X receptor agonist. Cancer Res. 2006;66:6482-6486.

23. Bensinger SJ, Bradley MN, Joseph SB, Zelcer N, Janssen EM, Hausner MA, Shih R, Parks JS, Edwards PA, Jamieson BD, Tontonoz P. LXR signaling couples sterol metabolism to proliferation in the acquired immune response. Cell. 2008;134:97-111.

24. Lo Sasso G, Celli N, Caboni M, Murzilli S, Salvatore L, Morgano A, Vacca M, Pagliani T, Parini P, Moschetta A. Down-regulation of the LXR transcriptome provides the requisite cholesterol levels to proliferating hepatocytes. Hepatology. 2010;51:1334-1344.

25. Guo D, Reinitz F, Youssef M, Hong C, Nathanson D, Akhavan D, Kuga D, Amzajerdi AN, Soto H, Zhu S, Babic I, Tanaka K, Dang J, Iwanami A, Gini B, Dejesus J, Lisiero DD, Huang TT, Prins RM, Wen PY, Robins HI, Prados MD,

Deangelis LM, Mellinghoff IK, Mehta MP, James CD, Chakravarti A, Cloughesy TF, Tontonoz P, Mischel PS. An LXR agonist promotes glioblastoma cell death through inhibition of an EGFR/AKT/SREBP-1/LDLR-dependent pathway. Cancer Discov. 2011;1:442-456.

26. Chinetti-Gbaguidi G, Staels B. Lipid ligand-activated transcription factors regulating lipid storage and release in human macrophages. Biochim Biophys Acta. 2009;1791:486–493.

27. Bensinger SJ, Tontonoz P. Integration of metabolism and inflammation by lipid-activated nuclear receptors. Nature. 2008;454:470–747.

28. Oosterveer MH, Grefhorst A, Groen AK, Kuipers F. The liver X receptor: control of cellular lipid homeostasis and beyond: implications for drug design. Prog Lipid Res. 2010;49:343–532.

29. Zhu M, Fu Y, Hou Y, Wang N, Guan Y, Tang C, Shyy JY, Zhu Y. Laminar shear stress regulates liver X receptor in vascular endothelial cells. Arterioscler Thromb Vasc Biol. 2008;28:527–533.

30. McLaren JE, Michael DR, Ashlin TG, Ramji DP. Cytokines, macrophage lipid metabolism and foam cells: implications for cardiovascular disease therapy. Prog Lipid Res. 2011;50:331–347.

31. Blaschke F, Leppanen O, Takata Y, Caglayan E, Liu J, Fishbein MC, Kappert K, Nakayama KI, Collins AR, Fleck E, Hsueh WA, Law RE, Bruemmer D. Liver X receptor agonists suppress vascular smooth muscle cell proliferation and inhibit neointima formation in balloon-injured rat carotid arteries. Circ Res. 2004;95:e110-123.

32. Schuster GU, Parini P, Wang L, Alberti S, Steffensen KR, Hansson GK, Angelin B, Gustafsson JA. Accumulation of foam cells in liver X receptor-deficient mice. Circulation. 2002;106:1147–1153.

33. 1. Bosch FX, Ribes J, Diaz M, Cleries R. Primary liver cancer: worldwide incidence and trends. Gastroenterology. 2004;127:S5–S16.

34. Lok AS. Prevention of hepatitis B virus-related hepatocellular carcinoma. Gastroenterology. 2004;127:S303–S309.

35. Cha C, Dematteo RP. Molecular mechanisms in hepatocellular carcinoma development. Best Pract Res Clin Gastroenterol. 2005;19:25–37.

36. Thomas MB, Zhu AX. Hepatocellular carcinoma: the need for progress. J Clin Oncol. 2005;23:2892–2899.

37. Lee DH, Kim JH, Nam JJ, Kim HR, Shin HR. Epidemiological findings of hepatitis B infection based on 1998 National Health and Nutrition Survey in Korea. J Korean Med Sci. 2002;17:457–462.

38. Ganem D, Prince AM. Hepatitis B virus infection-natural history and clinical consequences. N Engl J Med. 2004;350:1118–1129.

39. Fattovich G, Stroffolini T, Zagni I, Donato F. Hepatocellular carcinoma in cirrhosis: incidence and risk factors. Gastroenterology. 2004;127:S35–S50.

40. Park NH, Chung Y-H, Youn KH. Close correlation of p53 mutation to microvascular invasion in hepatocellular carcinoma. J Clin Gastroenterol. 2001;33:397–401.

41. Jiang J, Nilsson-Ehle P, Xu N. Influence of liver cancer on lipid and lipoprotein

metabolism. Lipids Health Dis. 2006;5:4.

42. Okuda K, Okuda H. Primary liver cell carcinoma. In: McIntyre N, Benhamou JP, Bircher J, Rizzetto M, Rodes, J, eds. Oxford textbook of clinical hepatology. Oxford University Press, Oxford. 1991:1019–1053.

43. Kanno T, Kurioka N, Kim S, Tamori A, Kim K, Oka H, Kuroki T, Mizoguchi Y, Kobayashi K. Implications of hyperechoic lesions in small hepatocellular carcinoma. Gastroenterology. 1989;24:528-534

44. Park US, Park SK, Lee YI, Park JG, Lee YI. Hepatitis B virus-X protein upregulates the expression of p21waf1/cip1 and prolongs G1 → S transition via a p53-independent pathway in human hepatoma cells. Oncogene. 2000;19(30):3384–3394.

45. Arbuthnot P, Capovilla A, Kew M. Putative role of hepatitis B virus X protein in hepatocarcinogenesis: effects on apoptosis, DNA repair, mitogen-activated protein kinase and JAK/STAT pathways. J Gastroenterol Hepatol. 2000;15:357-368.

46. Ng SA, Lee C. Hepatitis B virus X gene and hepatocarcinogenesis. J

Gastroenterol. 2011;46:974-990.

47. Murakami S. Hepatitis B virus X protein: a multifunctional viral regulator. J Gastroenterol. 2001;36:651-660.

48. Feitelson MA, Lee J. Hepatitis B virus integration, fragile sites, and hepatocarcinogenesis. Cancer Lett. 2007; 252: 157–170.

49. Leandro G, Mangia A, Hui J, Fabris P, Rubbia-Brandt L, Colloredo G. HCV Meta-Analysis (on) Individual Patients' Data Study Group., Relationship between steatosis, inflammation, and fibrosis in chronic hepatitis C: a meta-analysis of individual patient data. Gastroenterology. 2006;130:1636-1642.

50. Tsochatzis E, Papatheodoridis GV, Manesis EK, Chrysanthos N, Kafiri G, Archimandritis AJ. Hepatic steatosis in chronic hepatitis B develops due to host metabolic factors: a comparative approach with genotype 1 chronic hepatitis C. Dig Liver Dis. 2007;39:936-942.

51. Gordon A, McLean CA, Pedersen JS, Bailey MJ, Roberts SK. Hepatic steatosis in chronic hepatitis B and C: predictors, distribution and effect on fibrosis. J Hepatol.

2005;43:38-44.

52. Su AI, Pezacki JP, Wodicka L, Brideau AD, Supekova L, Thimme R. Genomic analysis of the host response to hepatitis C virus infection. Proc Natl Acad Sci U S A. 2002;26:15669-15674.

53. Moriishi K, Mochizuki R, Moriya K, Miyamoto H, Mori Y, Abe T. Critical role of PA28gamma in hepatitis C virus-associated steatogenesis and hepatocarcinogenesis. Proc Natl Acad Sci U S A. 2007;104:1661-1666.

54. He Y, Sun HQ, He XE, Wang WL, Lei JH. Knockdown of HBx by RNAi inhibits proliferation and enhances chemotherapy-induced apoptosis in hepatocellular carcinoma cells. Med Oncol. 2010 ;27:1227-1233.

55. Moriya K, Yotsuyanagi H, Shintani Y, Fujie H, Ishibashi K, Matsuura Y. Hepatitis C virus core protein induces hepatic steatosis in transgenic mice. J Gen Virol. 1997;78:1527-1531.

56. Fukasawa M, Tanaka Y, Sato S, Ono Y, Nitahara-Kasahara Y, Suzuki T. Enhancement of de novo fatty acid biosynthesis in hepatic cell line Huh-7 expressing

hepatitis C virus core protein. Biol Pharm Bull. 2006;29:1958-1961.

57. Yamaguchi A, Tazuma S, Nishioka T, Ohishi W, Hyogo H, Nomura S. Hepatitis C virus core protein modulates fatty acid metabolism and thereby causes lipid accumulation in the liver. Dig Dis Sci. 2005;50:1361-1371.

58. Idrees M, Riazuddin S. Frequency distribution of hepatitis C virus genotypes in different geographical regions of Pakistan and their possible routes of transmission. BMC Infect Dis 2008; 8:69.

59. Hajjou M, Norel R, Carver R, Marion P, Cullen J, Rogler LE. cDNA microarray analysis of HBV transgenic mouse liver identifies genes in lipid biosynthetic and growth control pathways affected by HBV. J Med Virol. 2005;77:57-65.

60. Kim KH, Shin HJ, Kim K, Choi HM, Rhee SH, Moon HB. Hepatitis B virus X protein induces hepatic steatosis via transcriptional activation of SREBP1 and PPARγ. Gastroenterology. 2007;132:1955-1967.

61. Kunjathoor VV, Febbraio M, Podrez EA, Moore KJ, Andersson L, Koehn S, Rhee JS, Silverstein R, Hoff HF, Freeman MW. Scavenger receptors class A-I/II and CD36

are the principal receptors responsible for the uptake of modified low density lipoprotein leading to lipid loading in macrophages. J Biol Chem. 2002;277:49982–49988.

62. Moore KJ, Kunjathoor VV, Koehn SL, Manning JJ, Tseng AA, Silver JM, McKee M, Freeman MW. Loss of receptor-mediated lipid uptake via scavenger receptor A or CD36 pathways does not ameliorate atherosclerosis in hyperlipidemic mice. J Clin Invest. 2005;115:2192–2201.

63. Manning-Tobin JJ, Moore KJ, Seimon TA, Bell SA, Sharuk M, varez-Leite JI, de Winther MP, Tabas I, Freeman MW. Loss of SR-A and CD36 activity reduces atherosclerotic lesion complexity without abrogating foam cell formation in hyperlipidemic mice. Arterioscler Thromb Vasc Biol. 2009;29:19–26.

64. Tabas I, Li Y, Brocia RW, Wu SW, Swenson TL, Williams KJ. Lipoprotein lipase and sphingomyelinase synergistically enhance the association of atherogenic lipoproteins with smooth muscle cells and extracellular matrix. A possible mechanism for low density lipoprotein and lipoprotein(a) retention and macrophage foam cell

formation. J Biol Chem. 1993;268:20419–20432.

65. Kruth HS, Jones NL, Huang W, Zhao B, Ishii I, Chang J, Combs CA, Malide D, Zhang WY. Macropinocytosis is the endocytic pathway that mediates macrophage foam cell formation with native low density lipoprotein. J Biol Chem. 2005;280:2352–2360.

66. Venkateswaran A, Laffitte BA, Joseph SB, Mak PA, Wilpitz DC, Edwards PA, Tontonoz P. Control of cellular cholesterol efflux by the nuclear oxysterol receptor LXR alpha. Proc Natl Acad Sci U S A. 2000;97:12097–12102.

67. Tangirala RK, Bischoff ED, Joseph SB, Wagner BL, Walczak R, Laffitte BA, Daige CL, Thomas D, Heyman RA, Mangelsdorf DJ, Wang X, Lusis AJ, Tontonoz P, Schulman IG. Identification of macrophage liver X receptors as inhibitors of atherosclerosis. Proc Natl Acad Sci U S A. 2002;99:11896–11901.

68. Teupser D, Kretzschmar D, Tennert C, Burkhardt R, Wilfert W, Fengler D, Naumann R, Sippel AE, Thiery J. Effect of macrophage overexpression of murine liver X receptor-alpha (LXR-alpha) on atherosclerosis in LDL-receptor deficient mice.

Arterioscler Thromb Vasc Biol. 2008;28:2009–2015.

69. Levin N, Bischoff ED, Daige CL, Thomas D, Vu CT, Heyman RA, Tangirala RK, Schulman IG. Macrophage liver X receptor is required for antiatherogenic activity of LXR agonists. Arterioscler Thromb Vasc Biol. 2005;25:135–142.

70. Bischoff ED, Daige CL, Petrowski M, Dedman H, Pattison J, Juliano J, Li AC, Schulman IG. Non-redundant roles for LXRalpha and LXRbeta in atherosclerosis susceptibility in low density lipoprotein receptor knockout mice. J Lipid Res. 2010;51:900–906.

71. Tabas I. Macrophage death and defective inflammation resolution in atherosclerosis. Nat Rev Immunol. 2010;10:36-46.

72. Woollard KJ, Geissmann F. Monocytes in atherosclerosis: subsets and functions. Nat Rev Cardiol. 2010;7:77-86.

73. Boström P, Magnusson B, Svensson PA, Wiklund O, Borén J, Carlsson LM, Ståhlman M, Olofsson SO, Hultén LM. Hypoxia converts human macrophages into triglyceride-loaded foam cells. Arterioscler Thromb Vasc Biol. 2006;26:1871-1876.

74. Savransky V, Jun J, Li J, Nanayakkara A, Fonti S, Moser AB, Steele KE, Schweitzer MA, Patil SP, Bhanot S, Schwartz AR, Polotsky VY. Dyslipidemia and atherosclerosis induced by chronic intermittent hypoxia are attenuated by deficiency of stearoyl coenzyme A desaturase. Circ Res. 2008;7:1173-1180.

75. Savransky V, Nanayakkara A, Li J, Bevans S, Smith PL, Rodriguez A, Polotsky VY. Chronic intermittent hypoxia induces atherosclerosis. Am J Respir Crit Care Med. 2007;15:1290-1297.

76. Li J, Nanayakkara A, Jun J, Savransky V, Polotsky VY. Effect of deficiency in SREBP cleavage-activating protein on lipid metabolism during intermittent hypoxia. Physiol Genomics. 2007;22:273-280.

77. Hughes AL, Todd BL, Espenshade PJ. SREBP pathway responds to sterols and functions as an oxygen sensor in fission yeast. Cell. 2005;25:831-842.

78. Jiang G, Li T, Qiu Y, Rui Y, Chen W, Lou Y. RNA interference for HIF-1alpha inhibits foam cells formation in vitro. Eur J Pharmacol. 2007;21:183-190.

79. Li J, Bosch-Marce M, Nanayakkara A, Savransky V, Fried SK, Semenza GL,

Polotsky VY. Altered metabolic responses to intermittent hypoxia in mice with partial deficiency of hypoxia-inducible factor-1alpha. Physiol Genomics. 2006;16:450-457.

80. Zelcer N, Tontonoz P. Liver X receptors as integrators of metabolic and inflammatory signaling. J Clin Invest. 2006;116:607-614.

81. Joseph SB, Tontonoz P. LXRs: new therapeutic targets in atherosclerosis? Curr Opin Pharmacol. 2003;3:192-197.

82. Watanabe Y, Jiang S, Takabe W, Ohashi R, Tanaka T, Uchiyama Y, Katsumi K, Iwanari H, Noguchi N, Naito M, Hamakubo T, Kodama T. Expression of the LXRalpha protein in human atherosclerotic lesions. Arterioscler Thromb Vasc Biol. 2005;25:622-627.

83. Rigamonti E, Chinetti-Gbaguidi G, Staels B. Regulation of macrophage functions by PPAR-alpha, PPAR-gamma, and LXRs in mice and men. Arterioscler Thromb Vasc Biol. 2008;28:1050-1059.

84. Grefhorst A, Elzinga BM, Voshol PJ, Plösch T, Kok T, Bloks VW, van der Sluijs FH, Havekes LM, Romijn JA, Verkade HJ, Kuipers F. Stimulation of lipogenesis by

pharmacological activation of the liver X receptor leads to production of large, triglyceride-rich very low density lipoprotein particles. J Biol Chem. 2002;13:34182-34190.

85. Chisholm JW, Hong J, Mills SA, Lawn RM. The LXR ligand T0901317 induces severe lipogenesis in the db/db diabetic mouse. J Lipid Res. 2003;44:2039-2048.

86. Yoo YG, Oh SH, Park ES, Cho H, Lee N, Park H, Lee MO. Hepatitis B virus X protein enhances transcriptional activity of hypoxia-inducible factor-1α through activation of mitogen-activated protein kinase pathway. J Biol Chem. 2003;278:39076-39084.

87. Yoo YG, Na TY, Seo HW, Seong JK, Park CK, Shin YK, Lee MO. Hepatitis B Virus X protein induces the expression of MTA1 and HDAC1, which enhances hypoxia signaling in hepatocellular carcinoma cells. Oncogene. 2008;27:3405-3413.

88. Lee MO, Kang HJ, Cho H, Shin EC, Park JH, Kim SJ. Hepatitis B virus X protein induced expression of the Nur77 gene. Biochem Biophys Res Commun. 2001 16;288(5):1162-1168.

89. Na TY, Shin YK, Roh KJ, Kang SA, Hong I, Oh SJ, Seong JK, Park CK, Choi YL, Lee MO. Liver X receptor mediates hepatitis B virus X protein-induced lipogenesis in hepatitis B virus-associated hepatocellular carcinoma. Hepatology. 2009;49:1122-1131.

90. Kim EJ, Yoo YG, Yang WK, Lim YS, Na TY, Lee IK, Lee MO. Transcriptional activation of HIF-1α by RORalpha and its role in hypoxia signaling. Arterioscler Thromb Vasc Biol. 2008;28:1796-1802.

91. Yoo YG, Kong G, Lee MO. Metastasis-associated protein 1 enhances stability of hypoxia-inducible factor-1alpha protein by recruiting histone deacetylase 1. EMBO J. 2006;22:1231-1241.

92. Stros M, Polanská E, Struncová S, Pospísilová S. HMGB1 and HMGB2 proteins up-regulate cellular expression of human topoisomerase IIalpha. Nucleic Acids Res. 2009;37:2070-2086.

93. Tanaka H, Yamamoto M, Hashimoto N, Miyakoshi M, Tamakawa S, Yoshie M, Tokusashi Y, Yokoyama K, Yaginuma Y, Ogawa K. Hypoxia-independent

overexpression of hypoxia-inducible factor 1alpha as an early change in mouse hepatocarcinogenesis. Cancer Res. 2006;1:11263-1170.

94. Dif N, Euthine V, Gonnet E, Laville M, Vidal H, Lefai E. Insulin activates human sterol-regulatory-element-binding protein-1c (SREBP-1c) promoter through SRE motifs. Biochem J. 2006;400:179-188.

95. Chavez JC, Baranova O, Lin J, Pichiule P. The transcriptional activator hypoxia inducible factor 2 (HIF-2/EPAS-1) regulates the oxygen-dependent expression of erythropoietin in cortical astrocytes. J Neurosci. 2006;13:9471-1981.

96. Schultz JR, Tu H, Luk A, Repa JJ, Medina JC, Li L, Schwendner S, Wang S, Thoolen M, Mangelsdorf DJ, Lustig KD, Shan B. Role of LXRs in control of lipogenesis. Genes Dev. 2000;15:2831-2838.

97. Repa JJ, Liang G, Ou J, Bashmakov Y, Lobaccaro JM, Shimomura I. Regulation of mouse sterol regulatory element-binding protein-1c gene (SREBP-1c) by oxysterol receptors, LXRα and LXRβ. Genes Dev. 2000;14:2819-2830.

98. Kim K, Kim KH, Kim HH, Cheong J. Hepatitis B virus X protein induces lipogenic transcription factor SREBP1 and fatty acid synthase through the activation of nuclear receptor LXR alpha. Biochem J. 2008;416:219-230

99. Oberkofler H, Schraml E, Krempler F, Patsch W. Potentiation of liver X receptor transcriptional activity by peroxisome-proliferator-activated receptor gamma co-activator 1 alpha. Biochem J. 2003;371:89-96.

100. Whitney KD, Watson MA, Goodwin B, Galardi CM, Maglich JM, Wilson JG, Willson TM, Collins JL, Kliewer SA. Liver X receptor (LXR) regulation of the LXRalpha gene in human macrophages. J Biol Chem. 2001;23:43509-43515.

101. Kuhajda FP. Fatty-acid synthase and human cancer: new perspectives on its role in tumor biology. Nutrition. 2000;16:202-208.

102. Menendez JA, Lupu R. Fatty acid synthase and the lipogenic phenotype in cancer pathogenesis. Nat Rev Cancer. 2007;7:763-777.

103. Yahagi N, Shimano H, Hasegawa K, Ohashi K, Matsuzaka T, Najima Y. Co-ordinate activation of lipogenic enzymes in hepatocellular carcinoma. Eur J Cancer.

2005;41:1316-1322

104. Kong HJ, Hong SH, Lee MY, Kim HD, Lee JW, Cheong J. Direct binding of hepatitis B virus X protein and retinoid X receptor contributes to phosphoenolpyruvate carboxykinase gene transactivation. FEBS Lett. 2000;483:114-118.

105. Ishizaka N, Ishizaka Y, Takahashi E, Toda Ei E, Hashimoto H, Ohno M. Increased prevalence of carotid atherosclerosis in hepatitis B virus carriers. Circulation. 2002;105:1028-1030.

106. Yoshikawa T, Shimano H, Yahagi N, Ide T, Amemiya-Kudo M, Matsuzaka T. Polyunsaturated fatty acids suppress sterol regulatory element-binding protein 1c promoter activity by inhibition of liver X receptor (LXR) binding to LXR response elements. J Biol Chem. 2002;277:1705-1711.

107. Tanaka N, Moriya K, Kiyosawa K, Koike K, Gonzalez FJ, Aoyama T. PPARalpha activation is essential for HCV core protein-induced hepatic steatosis and hepatocellular carcinoma in mice. J Clin Invest. 2008;118:683-694.

108. Jackel-Cram C, Babiuk LA, Liu Q. Up-regulation of fatty acid synthase promoter by hepatitis C virus core protein: genotype-3a core has a stronger effect than genotype-1b core. J Hepatol. 2007;46: 999-1008.

109. Mattsson L, Johansson H, Ottosson M, Bondjers G, Wiklund O. Expression of lipoprotein lipase mRNA and secretion in macrophages isolated from human atherosclerotic aorta. J Clin Invest. 1993;92:1759-1765.

110. Hultén LM, Lindmark H, Diczfalusy U, Björkhem I, Ottosson M, Liu Y, Bondjers G, Wiklund O. Oxysterols present in atherosclerotic tissue decrease the expression of lipoprotein lipase messenger RNA in human monocyte-derived macrophages. J Clin Invest. 1996;5:461-468.

111. Alkazemi D, Egeland G, Vaya J, Meltzer S, Kubow S. Oxysterol as a marker of atherogenic dyslipidemia in adolescence. J Clin Endocrinol Metab. 2008;93:4282-4289.

112. Brown AJ, Jessup W. Oxysterols and atherosclerosis. Atherosclerosis. 1999;142:1-28.

113. Mwaikambo BR, Yang C, Chemtob S, Hardy P. Hypoxia up-regulates CD36 expression and function via hypoxia-inducible factor-1- and phosphatidylinositol 3-kinase-dependent mechanisms. J Biol Chem. 2009;284:26695-26707.

114. Leonarduzzi G, Gargiulo S, Gamba P, Perrelli MG, Castellano I, Sapino A, Sottero B, Poli G. Molecular signaling operated by a diet-compatible mixture of oxysterols in up-regulating CD36 receptor in CD68 positive cells. Mol Nutr Food Res. 2010;54:S31-41.

115. Rydberg EK, Krettek A, Ullström C, Ekström K, Svensson PA, Carlsson LM, Jönsson-Rylander AC, Hansson GI, McPheat W, Wiklund O, Ohlsson BG, Hultén LM. Hypoxia increases LDL oxidation and expression of 15-lipoxygenase-2 in human macrophages. Arterioscler Thromb Vasc Biol. 2004;24:2040-2045.

116. Li Z, Wei H, Deng L, Cong X, Chen X. Expression and secretion of interleukin-1beta, tumour necrosis factor-alpha and interleukin-10 by hypoxia- and serum-deprivation-stimulated mesenchymal stem cells. FEBS J. 2010;277:3688-3698.

117. Bozza PT, Bandeira-Melo C. Mechanisms of leukocyte lipid body formation and

function in inflammation. Mem Inst Oswaldo Cruz. 2005;100:113-120.

118. Landis MS, Patel HV, Capone JP. Oxysterol activators of liver X receptor and 9-cis-retinoic acid promote sequential steps in the synthesis and secretion of tumor necrosis factor-alpha from human monocytes. J Biol Chem. 2002;15:4713-4721.

119. Walczak R, Joseph SB, Laffitte BA, Castrillo A, Pei L, Tontonoz P. Transcription of the vascular endothelial growth factor gene in macrophages is regulated by liver X receptors. J Biol Chem. 2004;12:9905-9911.

(국문 초록)

지질대사 이상 질환에서 핵 수용체 LXR 의 역할 및 기전에 대한 연구

나 태 영

약학과 병태생리학전공

서울대학교 대학원

고아 핵 수용체 Liver X Receptor (LXR)은 세포 내에 산화스테롤 (oxysterol)이 증가함에 따라 말초 조직에서 간으로 콜레스테롤을 운반하는 유전자들을 활성화 시켜 간의 지방 대사에 중요 인자로 알려져 있으며, 동맥경화와 고 콜레스테롤혈증 등의 병적인 상태에서 중요한 역할을 한다는 것이 알려져 왔다.

제 1 단원에서 B형 간염 바이러스 (Hepatitis B Virus, HBV)와 관련된 HBx에 의한 지방 간염에서의 LXRα/β 역할에 대하여 기술하였다. B형

간염 바이러스 감염 환자의 경우, 27%-51%의 환자에서 지방간이 진행될 정도로 HBV 감염과 지방간과의 연관성이 매우 높은 것으로 최근 논문들과 역학적 통계에 의해 알려지고 있었으나, B형 간염 바이러스에 의한 지방간과 간암과의 상관관계는 명확하게 밝혀진 바가 없었다. 먼저 HBx가 과 발현 되었을 경우, 간세포 내에 지방이 축적됨과 동시에 지질합성 관련 하위 유전자들의 발현이 증가되고 있음을 확인 할 수 있었다. 흥미롭게도 LXRs이 knock-down 되었을 때 LXR 하위 유전자들의 전사 활성이 억제되고 HBx에 따른 지질의 축적이 전혀 이루어지지 못하고 있음이 관찰되었다. LXRα는 HBx와 함께 핵 내에 존재하며 물리적인 상호작용을 하고 있음을 밝혔으며, HBx가 LXR 하위 유전자의 SREBP-1 프로모터에 CBP를 recruit 함으로써 LXR의 전사 활성을 유도하고 있었다. 마지막으로 HBx 과발현 형질 전환 마우스에서 생성된 지방간과 HBV 관련 간암 환자 조직에서 LXRβ와 target 유전자들의 발현이 유의적으로 높게 발현됨을 알았다. 따라서 HBx에 의한 LXR과 하위 유전자의 발현과 활성 증가가 HBV 감염에 의해 유도되는 지방간 생성과 간암 발생에 있어서

중요하다고 생각해 볼 수 있으며, B형 간염 바이러스에 의해 유도되는 지방간을 타겟으로 하는 새로운 치료 신약 개발을 유도하는 데에 중요한 자료가 될 것으로 판단되어진다.

제 2단원에서는 동맥 경화의 지질 발달에 있어서의 LXRα과 HIF-1α의 역할에 대하여 기술하였다. 동맥경화의 발단은 콜레스테롤을 포함한 대식세포 (macrophage), 즉 거품세포(foam cell)가 혈관벽에 축적되는 것이다. 또한, 혈관에서 저산소가 유도될 때 지질로 가득 찬 대식세포인 거품세포의 축적이 증가가 유도되어지고, 이는 동맥 경화를 발달시키는 중요한 인자로 작용할 수 있음이 기존 논문들에 의해 밝혀진 바 있다. 따라서 저산소 유도가 염증성 대식세포에서 지질 대사와 관련되어 LXR이 이를 매개하고 있는 지를 살펴보았다. 먼저 사람의 혈액으로부터 분리된 대식세포와 Raw264.7 대식세포주에서 LXR의 활성이 저산소에 의해 유도되며, 증가된 LXRα의 유도가 HIF-1α의 안정화와 전사 활성을 증가시킬 수 있다는 것을 밝혔다. 또한, LXRα와 HIF-1α가 핵 내에 존재하며, 물리적인 상호작용을 하고 있음을 밝혔으며, 이러한 LXRα와 HIF-1α의 상호작용이

대식세포에서 중성지질의 축적과 염증반응을 유도할 수 있음을 알아내었다. 이러한 결과들을 통해 LXRα와 HIF-1α 의 상호 전사 활성 기능과 HIF-1α 단백질 안정화에 있어서의 positive feed forward 조절이 대식세포에서의 거품세포 형성에 매우 중요한 역할을 하고 있음을 밝혔다.

주요어 : Hepatitis B Virus, HBx, Liver X Receptor, HBx, Hepatocellular carcinogenesis, Hepatosteatosis, Hypoxia, HIF-1α, Foam cell, Atherosclerosis

학번 : 2006-21966